Optimised induction of on-demand focal hippocampal and neocortical seizures by electrical stimulation

Sana Hannan<ce:contributor-role>Conceptualisation) (Data curation) (Formal analysis) (Investigation) (Methodology)<ce:contributor-role>Visualisation)<ce:contributor-role>Writing-original draft)<ce:contributor-role>Writing-review and editing), Mayo Faulkner (Investigation) (Methodology) (Resources) (Software), Kirill Aristovich (Formal analysis) (Resources) (Software), James Avery (Methodology) (Software), Matthew C. Walker (Methodology) (Supervision)<ce:contributor-role>Writing-review and editing), David S. Holder<ce:contributor-role>Conceptualisation) (Funding acquisition) (Supervision)<ce:contributor-role>Writing-review and editing)

PII: S0165-0270(20)30334-4

DOI: https://doi.org/10.1016/j.jneumeth.2020.108911

Reference: NSM 108911

To appear in: *Journal of Neuroscience Methods*

Received Date: 17 July 2020

Revised Date: 10 August 2020

Accepted Date: 12 August 2020

Please cite this article as: Hannan S, Faulkner M, Aristovich K, Avery J, Walker MC, Holder DS, Optimised induction of on-demand focal hippocampal and neocortical seizures by electrical stimulation, *Journal of Neuroscience Methods* (2020), doi: https://doi.org/10.1016/j.jneumeth.2020.108911

Type of article: Research Paper

Optimised induction of on-demand focal hippocampal and neocortical seizures by electrical stimulation

Sana Hannan [a*], Mayo Faulkner [b], Kirill Aristovich [a], James Avery [c], Matthew C. Walker [d] and David S. Holder [a]

[a] Department of Medical Physics and Biomedical Engineering, University College London, UK

[b] Wolfson Institute for Biomedical Research, University College London, UK

[c] Department of Surgery and Cancer, Imperial College London, UK

[d] UCL Queen Square Institute of Neurology, University College London, UK

Email: sana.hannan@ucl.ac.uk*

Highlights

- *In vivo* models of focal hippocampal and neocortical seizures are presented
- These are based on electrically stimulating brain regions of anaesthetised rats
- We optimised the stimulation parameters and anaesthetic to evoke seizures on demand
- Seizures were stereotypic, electrographically reproducible and reliably induced
- The models hold promise for neuroimaging studies and screening of antiseizure drugs

Abstract

Background

Epilepsy is a common neurological disorder affecting over 60 million people globally, approximately a third of whom are refractory to pharmacotherapy. Surgical resection of the epileptogenic zone is frequently unsuitable or ineffective, particularly for individuals with focal neocortical or mesial temporal lobe epilepsy. Therefore, there is a need to develop animal models for elucidating the mechanisms of focal epilepsies and evaluating novel treatment strategies.

New Method

We present two adapted *in vivo* seizure models, the neocortical and hippocampal epileptic afterdischarge models, that enable stereotyped seizures to be induced on demand by electrical stimulation in anaesthetised, neurologically intact rats. The stimulation parameters and anaesthetic were optimised to generate electrographically reproducible, self-sustaining seizures with a well-defined focal origin.

Results

Neocortical or hippocampal seizures were consistently generated under fentanyl-isoflurane anaesthesia by stimulating the sensorimotor cortex or perforant path, respectively, with 100 Hz trains of biphasic

square-wave pulses. The induced seizures were suppressed by propofol, an established antiseizure anaesthetic, thus validating the clinical responsiveness of the developed models.

Comparison with Existing Methods

The high degree of reproducibility in seizure presentation, predictable seizure induction and ability to operate in anaesthetised animals renders these models overall less laborious and more cost-effective than most conventionally used seizure models.

Conclusions

The proposed models provide an efficient method for the high-throughput screening of novel antiseizure therapies, including closed-loop stimulation paradigms, and are well-suited to *in vivo* investigations that require tight regulation of seizure timing under anaesthetised conditions, particularly neuroimaging studies aimed at understanding the development of epileptogenic networks.

Keywords: seizure, epilepsy, animal model, rat, neocortex, hippocampus, anaesthetic, electrical stimulation

Submitted to: Journal of Neuroscience Methods

1. Introduction

1.1. Background

Epilepsy is one of the most prevalent chronic neurological disorders worldwide and affects over 60 million people globally (Ngugi, et al., 2010). Despite receiving optimal treatment, approximately 30% of individuals with epilepsy are refractory to the available anticonvulsant medication (Nair, 2016). Surgical resection of the epileptogenic zone is presently suitable for fewer than 5% of patients with refractory epilepsy (Lhatoo, et al., 2003). Mesial temporal lobe epilepsy (mTLE), frequently characterised by a seizure onset within the hippocampal formation, is the most common of the human focal epilepsies and represents the majority of cases of refractory epilepsy managed surgically (Cendes, 2005; Cross & Cavazos, 2009; Blair, 2012). However, seizure relapse ≥1 year post-surgery, following an initial seizure-free period, occurs significantly more in individuals with mTLE compared to other epilepsy syndromes (Spencer, 1996; Hennessy, et al., 2000; Spencer, et al., 2003). In focal neocortical epilepsy (FNE), on the other hand, surgical intervention is often limited by the high risk of postoperative neurological deficits if the epileptogenic zone is localised to eloquent regions of the cortex or the surrounding areas (Schuele & Lüders, 2008). There is, therefore, an urgent need to improve our understanding of the complex interplay between structural and functional abnormalities underlying these conditions and develop alternative treatment options.

Animal models of seizures and epilepsy are invaluable tools for supporting studies aimed at elucidating the mechanisms of epileptogenesis and testing novel antiseizure treatments. The majority of acute seizure models used for antiseizure drug testing involve systemic convulsants or generalised electrical stimulation (Smith, et al., 2007). The most commonly used rodent models of focal epilepsies involve the generation of spontaneous recurrent seizures following initial status epilepticus, and a subsequent period of latency, or kindling (Kandratavicius, et al., 2014). These models typically rely on the local or systemic administration of chemoconvulsants, such as kainic acid or pilocarpine (Ben-Ari, 1985; Curia, et al., 2008), or the repeated electrical stimulation of a specific brain region to evoke a progressive enhancement of its susceptibility to chronic spontaneous seizures (Sayin, et al., 2003; Kandratavicius, et al., 2014). Although these models can provide clinically realistic representations of several features of human epilepsies, they may be unsuitable for use in the initial assessment of novel treatment options (Löscher, 2017). This is because the induced spontaneous recurrent seizures are often infrequent and therefore challenging to capture. As such, video-EEG monitoring for several weeks is usually required to evaluate the potential anticonvulsant effects of a given therapeutic intervention, making the process laborious, time-consuming and inefficient (Kowski & Holtkamp, 2015). Thus, there is a need to develop animal models of focal seizures, such as those that occur in mTLE and FNE, that enable induction of stereotyped neocortical or limbic seizures on demand and are highly predictive of the clinical response to novel therapies.

In vivo epilepsy models also present unique challenges for neuroimaging studies that are aimed at improving our understanding of seizure propagation and the development of epileptogenic networks. Many neuroimaging methods used for studying these mechanisms, including electrical impedance tomography (EIT) and functional MRI (fMRI), typically require: (a) tight regulation of seizure induction to ensure adequate data acquisition during imaging protocols; (b) anaesthetisation and paralysis of the animal to eliminate movement artefacts during seizures; and (c) a high degree of reproducibility in the localisation of seizure foci and electrographic features of seizures within and across animals to enable assessment of the accuracy of reconstructions (Blumenfeld, 2007; Airaksinen, et al., 2011; Vongerichten, et al., 2016; Hannan, et al., 2018a).

The epileptic afterdischarge (AD) model holds potential to fulfil these criteria. In this model, specific brain regions of neurologically intact, non-epileptic animals are electrically stimulated to induce focal patterns of epileptiform activity without prior kindling or administration of chemoconvulsants (Kandratavicius, et al., 2014). The electrographic features of the induced epileptiform events depend principally on the area of the brain undergoing repetitive stimulation. For example, stimulating the prefrontal cortex of awake rats with a 5-s train of 50 Hz pulses, each 0.5 ms in duration with 600-800 µA current, induces epileptiform ADs of a spike-and-wave nature which subsequently propagate to the hippocampus and nucleus accumbens (Ma & Leung, 2010). Similarly, electrical stimulation of the sensorimotor cortex in rats with 15-s trains of biphasic rectangular pulses, each 1 ms in duration at 8 Hz, is an established method of producing spike-and-wave rhythms as well as clonic seizures restricted to facial and forelimb muscles in freely moving rats (Kubová & Mares, 1995; Kubová, et al., 1996; Polásek, et al., 1996; Haugvicová, et al., 2002). Such neocortical epileptiform events are characterised by synchronous rhythmic spikes and spike-wave complexes immediately after stimulation and typically last 5-85 s (Nelson, et al., 2010). Additionally, several studies have targeted limbic structures for electrically-induced ADs, which tends to generate higher frequency, large-amplitude epileptiform events (Bragin, et al., 1997; Norwood, et al., 2010). For example, repetitive electrical stimulation of the perforant path, the major excitatory input to the hippocampus, elicits epileptiform activity characterised by an initial primary AD of oscillations with a range of frequency bands collectively ranging from 2-400 Hz, followed by a silent postictal refractory period and a subsequent secondary AD consisting of fast oscillations of a lower amplitude at 40-80 Hz (Leung, 1987; Buzsàki, et al., 1989; Bragin, et al., 1997; Kandratavicius, et al., 2014).

Although epileptic AD models of epilepsy allow for stereotypic epileptiform events to be induced on demand, they typically use awake, freely moving animals and thus may be limiting for neuroimaging applications, which often require animals to be anaesthetised (Blumenfeld, 2007; Airaksinen, et al., 2011; Vongerichten, et al., 2016; Hannan, et al., 2018a). This can be problematic as many general anaesthetic agents are known to suppress epileptiform activity in the rat brain (van Luijtelaar, et al., 2002; Sleigh, et al., 2009; Airaksinen, et al., 2011; Kenny, et al., 2014; Hannan, 2019). The present study was therefore aimed at adapting and optimising the epileptic AD models to induce epileptiform events under general anaesthesia. This was intended primarily to provide a method for evaluating the technical accuracy of EIT, an emerging imaging modality, for imaging fast electrical activity during epileptiform events *in vivo*. EIT is able to image fast impedance changes which arise during neural activity with high spatiotemporal resolution through the rat cerebral cortex, using non-penetrating epicortical electrodes, and therefore represents a novel method for understanding neuronal network dynamics in epilepsy (Aristovich, et al., 2016). Prior to proceeding with these investigations, however, it was necessary to assess the localisation accuracy, depth resolution and limitations of the technique, which required a working model of reproducible and well-characterised neocortical and hippocampal epileptiform events that are induced electrically and can operate under anaesthetised conditions. Such a model would also be advantageous for use in any other *in vivo* investigation into seizure propagation and screening of novel therapies that require controlled seizure timing in an acute experimental setup.

1.2. Purpose

The purpose of this study was to develop the neocortical and hippocampal epileptic AD models to induce stereotypic epileptiform events on demand in anaesthetised rats. The requirement was to generate ictal events that had a well-defined focal origin within the neocortex or hippocampus and exhibited a high degree of reproducibility. We aimed to: (a) establish the optimal electrical stimulation parameters and anaesthetic agent needed to achieve this; (b) characterise the electrographic properties

of the resulting epileptiform events; and (c) evaluate the potential of the developed models for *in vivo* experimental and pre-clinical research.

1.3. Experimental design

For the neocortical epileptic AD model, the stimulated region within the cortex was the primary sensorimotor area at the boundary between the primary motor cortex and the hindlimb (HL) representation within the primary somatosensory cortex (M1/S1 HL), consistent with previous studies which have employed this model (Kubová & Mares, 1995; Kubová, et al., 1996; Polásek, et al., 1996; Haugvicová, et al., 2002; Nelson, et al., 2010). In the hippocampal epileptic AD model, stimulation was directed to the angular bundle of the perforant path, the major afferent projection into the hippocampus (Vicedomini & Nadler, 1987; Bragin, et al., 1997; Walker, et al., 1999; Langberg, et al., 2016). The perforant path originates in the entorhinal cortex and terminates on granule cells in the dentate gyrus, the input region of the hippocampus, in which epileptiform discharges are expected to occur in this model (Shepherd, 2004). Based on the previous studies that have used these models in freely-moving rats, the parameters of electrical stimulation to test were: pulse waveform, pulse width, pulse amplitude, frequency of stimulation and duration of stimulus train. The time interval between stimulus trains was also optimised as ictal events are often followed by an electrically quiescent, refractory state which diminishes over time. A minimum inter-train interval of 7 min was used to prevent kindling of neural circuits due to repeated stimulation and thus ensure that seizure patterns remained consistent during experiments (Nelson, et al., 2010).

The choice of anaesthetic was an important consideration since the majority of previous studies utilising the epileptic AD model had used awake, freely moving rats (Kubová, et al., 1996; Bragin, et al., 1997; Krupp & Löscher, 1998; Velísek & Mares, 2004; Nelson, et al., 2010; Fábera & Mares, 2014). In all experiments, anaesthesia was induced and maintained with isoflurane until after completion of surgery due to its ease of use, relatively short half-life which enables greater control over depth of anaesthesia, and uncommon rates of overdose compared to many intraperitoneally administered agents based on prior in-house experience. For the subsequent maintenance of anaesthesia during model development, α-chloralose and fentanyl were tested, in different animals, to determine which of these agents was most permissive to the induction of epileptiform events. α-chloralose is a widely used anaesthetic in neuroscientific research due to its presumed minimal depression of autonomic function (Luckl, et al., 2008; Flecknell, 2015). It is also known to have stimulatory effects on the central nervous system (CNS) and has been described as a convulsant, evidenced by the manifestation of myoclonic jerks during its use (Rosenbluth & Cannon, 1942; Winters & Spooner, 1966). Furthermore, the enhancement of electrically-induced cortical ADs with α-chloralose has been previously demonstrated in rabbits (Rao, 2000). For these reasons, α-chloralose was considered an appropriate initial choice for developing the epileptic AD models. A second agent considered for the maintenance of general anaesthesia, in case epileptiform events could not be induced under α-chloralose, was fentanyl. A potent narcotic analgesic, fentanyl works primarily by agonising μ-opioid receptors and is known to be permissive to the manifestation of epileptiform discharges both clinically and in numerous rat models of epilepsy (Schwark, et al., 1986; Tempelhoff, et al., 1992; Manninen, et al., 1999; Sanabria, et al., 2006; Hunfeld, et al., 2013). These pro-convulsant properties, together with a short half-life and duration of action due to its highly lipophilic nature (Pathan & Williams, 2012), made fentanyl an attractive alternative for use in this study. However, fentanyl alone does not provide sufficient anaesthesia and so is often used in combination with droperidol (Hunfeld, et al., 2013) or inhalational anaesthetics such as isoflurane (Muñoz, et al., 2005).

In the neocortical epileptic AD model, a 57-electrode epicortical array was implanted to: (a) enable electrical stimulation of the sensorimotor cortex for inducing epileptiform events; and (b) provide extensive coverage of the cortical surface to obtain ECoG recordings to confirm the presence of ictal discharges and monitor their propagation through the cortex. In the hippocampal model, in addition to an epicortical array, intracranial stimulating and recording depth electrodes were required to induce epileptiform events in the hippocampus and validate their presence with local field potential (LFP) recordings, respectively. The LFP probe contained 16 recording sites spaced 100 µm apart, thus allowing for high-resolution monitoring of epileptiform activity and precise determination of the ictal focus. In the following sections, the electrically-induced epileptiform events will be referred to as 'seizures'. To validate the clinical responsiveness of the developed models, the effect of propofol on the ability to induce seizures was assessed. Propofol, a general anaesthetic that acts primarily by enhancing gamma-aminobutyric acid type A ($GABA_A$) receptor function, has established antiseizure properties and is routinely used for the control of refractory status epilepticus in humans (Wood, et al., 1988; McBurney, et al., 1993; Stecker, et al., 1998; Shorvon & Ferlisi, 2011). Thus, by determining whether the models were predictive of the clinical response to propofol, their potential for use in the testing of novel antiseizure therapies could be evaluated.

2. Materials and Methods

2.1. Animal preparation

All animal handling and experimental investigations undertaken in this study were ethically approved by the UK Home Office and performed in accordance with its regulations, as outlined in the Animals (Scientific Procedures) Act 1986. Ten adult female Sprague-Dawley rats (300-450 g) were used in total. The use of female rats in our study, which reduced overall animal usage within the UCL Biological Services Unit, complied with the 3Rs principles (Reduction, Refinement and Replacement) of the Animal (Scientific Procedures) Act 1986. Prior to experiments, all rats were housed in standard Plexiglas cages in groups of up to three with a 12-hour light/dark cycle and given *ad libitum* access to food and water. Anaesthesia was induced with 4% isoflurane (inspired concentration) in 2 $Lmin^{-1}$ O_2 and an endotracheal intubation was performed to enable mechanical control of ventilation with 1.5-3% isoflurane in a 30/70 mixture of oxygen/air using an SAV03 small animal ventilator (Vetronic Services Ltd, Abbotskerswell, UK). Cannulation of the right femoral vessels was undertaken to allow for monitoring of intra-arterial blood pressure and intravenous access. Exhaled gases, respiratory rate, tidal volume, heart rate, invasive arterial blood pressure and SpO_2 were monitored regularly using an anaesthetic monitor (Lightning; Vetronic Services Ltd., Abbotskerswell, UK) and core body temperature was maintained at 36.5 ± 0.5 ºC using a homeothermic heating unit (Harvard Apparatus, Edenbridge, UK).

2.2. Surgery and electrode implantation

Rats were head-fixed in a stereotactic frame (Narishige International Ltd., London, UK) in the prone position using blunt-tipped interaural and incisor bars, and the skull was exposed by incising the scalp and displacing the skin of the head. The insertion of the temporal muscle was cauterised using a bipolar coagulation unit (Codman Malis CMC-II; Codman, Raynham, MA) and incised with a scalpel. Throughout the craniotomy, durotomy and electrode implantation procedures, the brain was kept moist by frequent irrigation with sterile saline (0.9% NaCl) at 37 ºC.

2.2.1. Neocortical epileptic AD model

Seven rats were required to develop the acute neocortical epileptic AD model. In each of these, a wide trapezoidal craniotomy was performed on one hemisphere using a veterinary bone drill (Ideal Micro-Drill; Harvard Apparatus, Edenbridge, UK). The paramedial edge of the craniotomy extended from 1 mm anterior to lambda to 5 mm posterior to bregma, with the lateral boundary at the junction of the zygomatic arch and the temporal bone, forming a trapezoidal opening. The dura was then incised to enable implantation of a planar 57-contact epicortical electrode array, fabricated from stainless steel foil and silicone rubber, on the exposed cortical surface. The array, which measured 15x9 mm at its furthest edges and contained 57 circular electrode contacts, each 0.6 mm in diameter, has been used previously (Faulkner, et al., 2018a; Faulkner, et al., 2018b; Hannan, et al., 2018a; Hannan, et al., 2018b).

2.2.2. Hippocampal epileptic AD model

The hippocampal epileptic AD model was developed using three rats. In two of these rats, two small rounded craniotomies (≥2 mm), centred on the positions of the stimulating and recording depth electrodes, were made in the left hemisphere. Following dura removal, the two depth electrodes were stereotactically positioned to be orthogonal to the exposed cortical surface and implanted into their target structures using micromanipulators (SM-15; Narishige International Ltd., London, UK). The stimulating electrode consisted of two twisted polydimide-insulated stainless steel wires (bare wire diameter: 125 μm; outer diameter: 203 μm) with 0.5 mm vertical tip separation (MS303/3- A/SPC;

Plastics One Inc., Roanoke, VA, USA) and targeted the left angular bundle to stimulate the perforant path projection from Layer II/III of the entorhinal cortex (AP = -8.1, ML = 4.4, DV = 3.5 mm from cortical surface; AP and ML given with respect to bregma). The recording depth electrode was a 16-channel linear silicon probe (A1x16-10mm-100-703; NeuroNexus Technologies Inc., Ann Arbor, MI, USA). The 16 iridium electrode contacts, each 30 μm in diameter, had a centre-to-centre spacing of 100 μm and spanned a total length of 1.5 mm. This depth probe was directed to the granule cell layer of the dentate gyrus of the hippocampus (AP = -4.0, ML = 2.5, DV = 2.8-4.0 mm from cortical surface) for recording LFPs to determine the presence of hippocampal epileptiform discharges following stimulation.

In the third rat, a wide trapezoidal craniotomy was performed to enable implantation of a modified planar epicortical array, containing 54 electrodes and two rectangular apertures centred on the positions of the stimulating and recording depth electrodes, described previously (Hannan, et al., 2020). The depth electrodes were advanced through the array and stereotactically implanted in the same positions as above. As such, ECoG recordings could be obtained simultaneously to depth recordings to confirm that the induced epileptiform activity was indeed localised to the hippocampus.

2.3. Maintenance of anaesthesia

2.3.1. Neocortical epileptic AD model

Following electrode implantation, either α-chloralose or fentanyl was introduced intravenously for the maintenance of anaesthesia. In the first four rats, a 60 mg/kg bolus of 1% w/v α-chloralose (Sigma-Aldrich, Dorset, UK), in 0.9% w/v NaCl, was administered intravenously over 30 min to prevent hypervolemia due to overload of fluid in the venous system. Anaesthesia was subsequently maintained by continuous infusion at 20 mg/kg/h. Over the course of the 30-60 min period after introducing α-chloralose, the rat was gradually weaned off isoflurane. A period of at least 1 hour was allowed after discontinuing isoflurane anaesthesia before cortical stimulation was started, in accordance with blood oxygen level-dependent functional MRI (BOLD-fMRI) studies which have utilised isoflurane and α-chloralose in a similar manner to measure haemodynamic responses associated with somatosensory evoked potentials (SEPs) (Sommers, et al., 2009; Tsurugizawa, et al., 2010).

Epileptiform discharges could not be induced in animals under α-chloralose anaesthesia, despite extensively varying the stimulation parameters; thus, the remaining three rats used to develop the neocortical model received fentanyl. In these rats, anaesthesia was maintained with continuously infused intravenous fentanyl at 20 μg/kg/h (Eurovet Animal Health Ltd., Cambridge, UK). After introducing fentanyl, the isoflurane concentration was gradually reduced to ~0.5%.

2.3.2. Hippocampal epileptic AD model

In all rats used to develop the hippocampal epileptic AD model, anaesthesia was maintained after electrode implantation with continuously infused fentanyl at 20 μg/kg/h and ~0.5% isoflurane, as this anaesthetic combination had enabled reliable seizure induction in the neocortical epileptic AD model which was optimised first.

2.4. Seizure induction

2.4.1. Neocortical epileptic AD model

Two electrodes within the 57-electrode epicortical array, each 0.6 mm in diameter, were used to stimulate the sensorimotor cortex to induce seizures. The positions of the stimulating electrodes were

determined by functionally mapping the forelimb and hindlimb representations in the primary somatosensory cortex. To do this, SEPs were elicited by electrically stimulating peripheral nerves (medial, ulnar and radial) in the contralateral forelimb and hindlimb with 1 mA monopolar square-wave pulses, 0.5 ms in duration, at a frequency of 2 Hz using a Neurolog current stimulus isolator (NL800A; Digitimer Ltd, Welwyn Garden City, UK). The resulting SEPs were recorded from the somatosensory cortex with the epicortical electrode array and averaged over 30 s (60 averages). The ECoG channels exhibiting the highest-amplitude forelimb and hindlimb SEPs were considered to be positioned at the centre of the forelimb or hindlimb representation, respectively (Fig. 1). The sensorimotor cortex, defined as the boundary between the hindlimb somatosensory and motor cortex (M1/S1 HL), was located accordingly. The two electrodes either side of the sensorimotor cortex, with a centre-to-centre distance of 2.6 mm, were stimulated with the parameters described below to evoke reproducible seizures in the neocortex (Fig. 1). The amplitudes and latencies of recorded SEPs were also assessed to confirm that the cerebral cortex was in a functionally normal condition prior to commencing cortical stimulation.

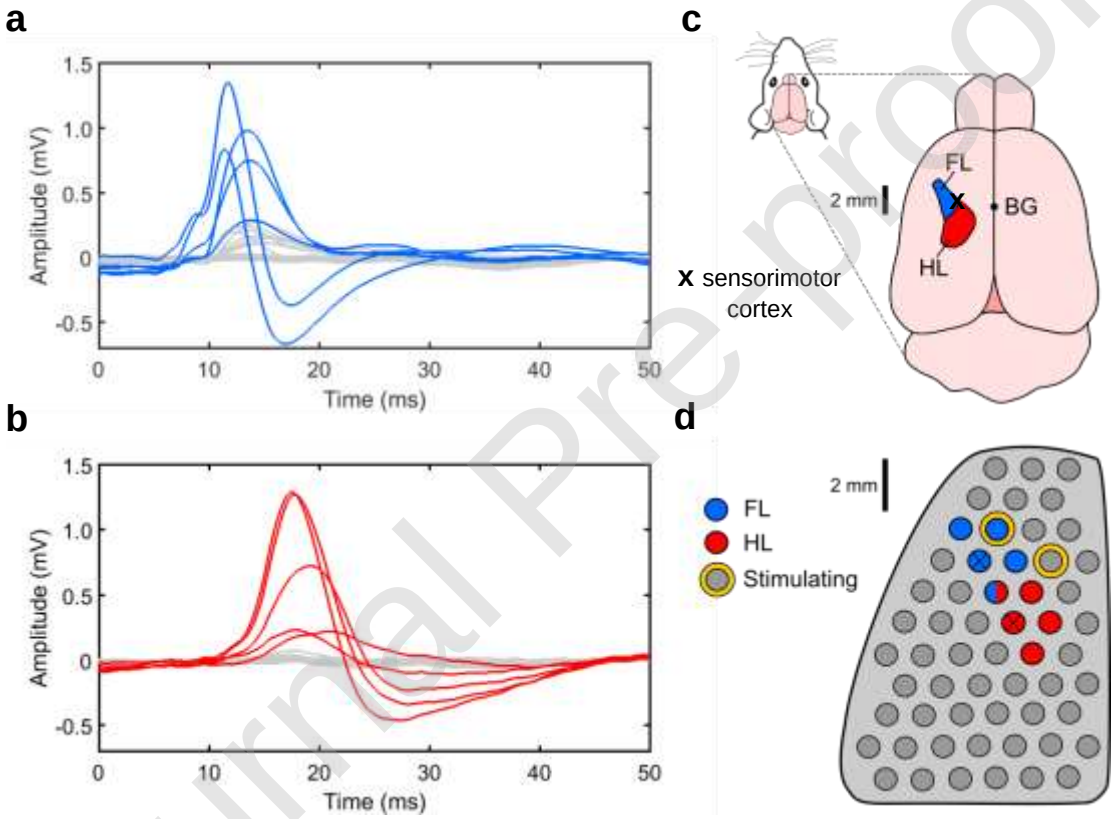

Figure 1. Functional localisation of stimulation site for neocortical epileptic AD model. Representative examples of averaged forelimb (FL) (**a**) and hindlimb (HL) (**b**) SEPs induced by delivery of a FL or HL stimulus at 0 ms and recorded from the surface of the cerebral cortex. (**d**) The electrodes on the 57-electrode epicortical array from which the five highest-amplitude peaks were recorded for each evoked response are indicated, with the channels corresponding to largest SEPs marked with an 'X'. With reference to a map of the FL and HL representations within the rat somatosensory cortex on which the sensorimotor region is indicated, given with respect to bregma (BG) (**c**), this information was used to determine the positions of the two electrodes for stimulating the sensorimotor cortex (**d**). The two stimulating electrodes were positioned either side of the sensorimotor cortex and separated by a centre-to-centre distance of 2.6 mm; based on prior in-house modelling, this ensured that there would be a sufficiently high current density within the sensorimotor region for inducing epileptiform discharges.

A wide range of electrical stimulation parameters were tested across the seven rats until neocortical seizures could be induced reliably (Table 1). Three types of stimulus waveforms, all rectangular in shape, were used overall: (a) biphasic symmetric, consisting of a charge- and time-balanced pulse; (b) biphasic asymmetric, comprising a charge-balanced pulse with an initial positive component, the duration of which was a fifth of the total pulse duration (that is, a short high-amplitude depolarising period preceding a prolonged low-amplitude hyperpolarisation period); or (c) monophasic (Fig. 2). Pulses were applied at frequencies of 8, 50 or 100 Hz in stimulus trains lasting 0.5-15 s. Pulse widths that were used, defined as the duration of the positive component of the waveform, ranged from 0.1-2 ms. For each combination of these parameters, the amplitude of applied current and time interval between stimulus trains were the main variables. Stimulation was commenced at 100 μA and increased in increments of 0.1-1 mA to a maximum applied current of 15 mA until ictal discharges, defined as sharp spikes <70 ms in duration with a peak-to-peak amplitude of ≥2 mV, could be observed in the ECoG traces. Inter-train intervals ranged from 7 to 20 min. The current threshold required to elicit ADs is expected to be variable across animals due to age and weight differences (Kubová, et al., 1996; Krupp & Löscher, 1998). All stimulus pulses tested were driven by the Keithley 6221 current source (Keithley Instruments Ltd, Solon, OH, USA), controlled by custom written software in MATLAB (The MathWorks, Inc., Natick, MA, USA). If motor manifestations of seizures were severe enough to produce artefacts in ECoG recordings, rats were paralysed by administering pancuronium bromide (1 mg/kg i.v.).

Model	**Anaesthetic**	**Stimulation parameters**					
		Pulse waveform	**Pulse width (ms)**	**Frequency (Hz)**	**Train duration (s)**	**Amplitude (mA)**	**Inter-train interval (min)**
Neocortical epileptic AD model	α-chloralose, fentanyl-isoflurane	Biphasic symmetric, biphasic asymmetric and monophasic square-wave pulses	0.1-2	8, 50, 100	0.5-15	0.1-15	7-20
Hippocampal epileptic AD model	Fentanyl-isoflurane	Biphasic symmetric square-wave pulses	0.1, 1	100	2, 5	0.5-2	7-20

Table 1. Stimulation parameters and anaesthetics tested for the neocortical and hippocampal epileptic AD models. A narrower range of parameters of electrical stimulation, and only the fentanyl-isoflurane anaesthetic combination, needed to be tested to optimise the hippocampal model because the neocortical model was developed first.

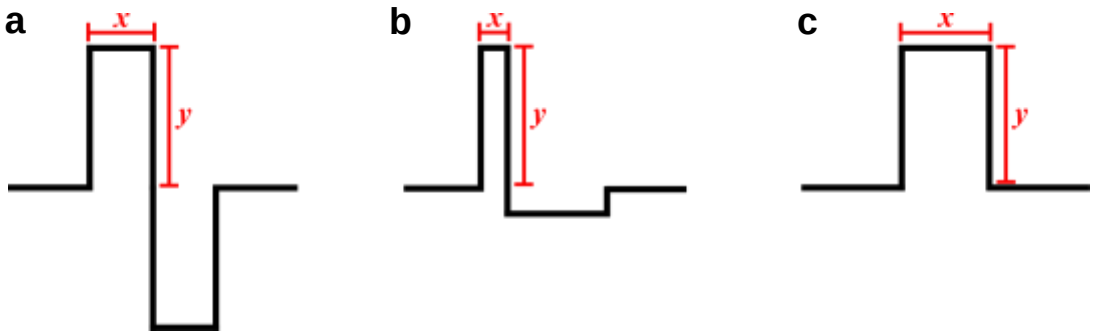

Figure 2. Pulse waveforms for cortical stimulation. Biphasic symmetric (**a**), biphasic non-symmetric (**b**), and monophasic (**c**) stimulus pulses were tested. Pulse width (*x*) defines the duration of the positive component of each waveform. Pulse width and amplitude of applied current (*y*) were varied over 0.1-2 ms and 0.1-15 mA, respectively.

2.4.2. Hippocampal epileptic AD model

To confirm that the stimulating and recording depth electrodes were positioned correctly, evoked activity comprising a granule cell population spike superimposed on a field excitatory postsynaptic potential (EPSP) was induced in the dentate gyrus by delivering 1 mA monopolar square-wave pulses, 150 μs in duration, to the stimulating electrode at a frequency of 0.5 Hz using a Neurolog current stimulus isolator (Fig. 3). The resulting evoked responses were recorded from the hippocampus with the 16-electrode depth probe and averaged over 2 min. Once the expected activity was observed, the depth probe was gradually advanced ventrally, in 0.1 mm intervals, until the highest-amplitude population spikes were recorded by the central electrodes within the probe (Fig. 3c,d). After validating the correct placement of the depth electrodes using these confirmatory LFP recordings, testing of parameters for inducing hippocampal epileptiform activity was commenced.

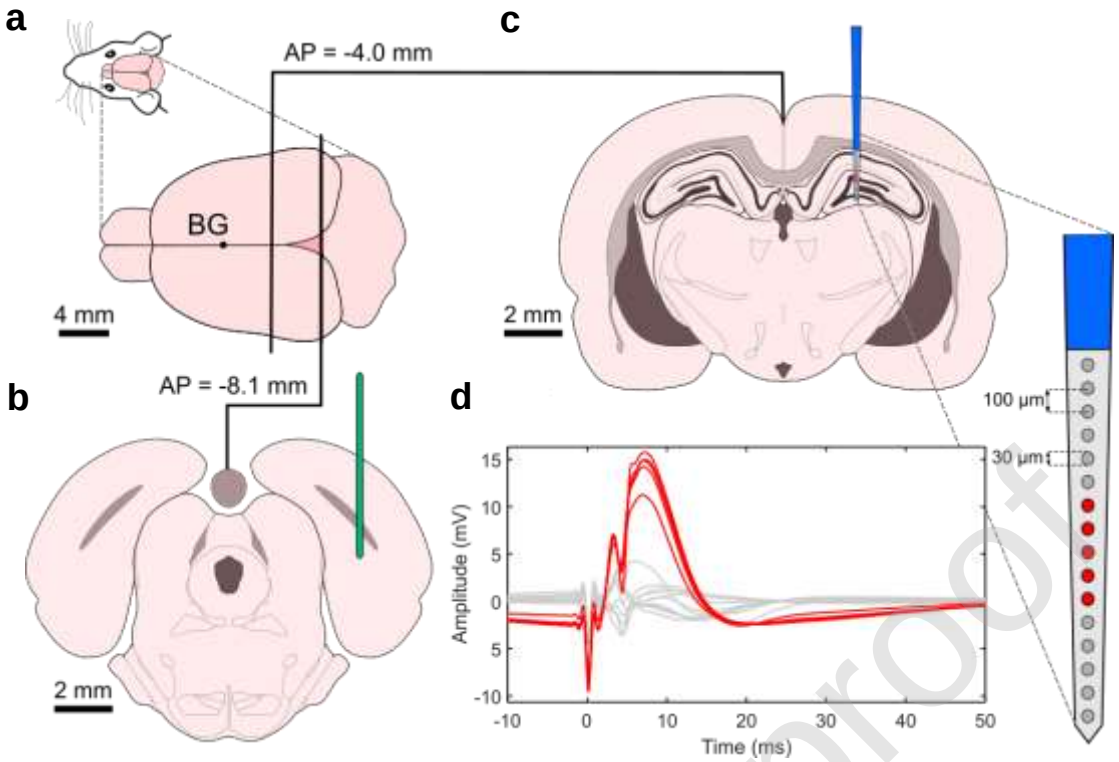

Figure 3. Functional validation of stimulating and recording depth electrode positions for hippocampal epileptic AD model. (**a**) Coronal sections obtained at -8.1 and -4.0 mm anteroposterior (AP) to bregma (BG) are provided to show the targeted positions of the stimulating and recording depth electrodes, respectively. (**b**) A twisted wire bipolar stimulating electrode (green) was implanted into the left angular bundle to target the perforant path projection from Layer II/III of the entorhinal cortex. (**c**) A 16-channel neural depth probe was directed to the granule cell layer of the dentate gyrus, the input region of the hippocampus, for recording. (**d**) To confirm the correct placement of depth electrodes, evoked activity was induced in the dentate gyrus by delivering 1 mA monopolar square-wave pulses to the stimulating electrode at 0.5 Hz. A representative example of recordings of this evoked activity, averaged over 60 trials, is displayed, with each trace recorded by an individual electrode contact on the depth probe. Negative-going dentate granule cell population spikes (peak at ~4 ms) superimposed on positive-going field EPSPs (peak at ~7 ms) can be seen, with respect to the stimulation artefact at 0 ms. The recording depth probe was advanced ventrally until the five electrodes corresponding to the highest-amplitude population spikes, marked in red, were positioned in the central portion of the probe. Schematic illustrations of coronal sections are adapted from Paxinos and Watson's stereotactic atlas of the rat brain (Paxinos & Watson, 2013).

Since the neocortical epileptic AD model was developed first, a narrower range of stimulus parameters needed to be tested to obtain a working model of hippocampal seizures in the anaesthetised rat (Table 1). Two main stimulation protocols were tested, both involving biphasic, symmetric pulses directed to the angular bundle of the perforant path. The first (protocol 1) involved delivery of a 5-s train of pulses, with a pulse width of 0.1 ms, to the stimulating electrode at a frequency of 100 Hz using a Keithley 6221 current source. In the second protocol (protocol 2) the pulses had a pulse width of 1 ms and were applied at 100 Hz for a total duration of 2 s. For each protocol, the amplitude of applied current was varied between 0.5 and 2 mA and the range of inter-train intervals tested was 7-20 min.

2.5. Evaluating the effects of propofol on seizure induction

The clinical responsiveness of the optimised models was validated by assessing their ability to induce neocortical and hippocampal seizures following administration of propofol, an established antiseizure anaesthetic used for the clinical suppression of seizures (Wood, et al., 1988). After completing electrophysiological recordings for seizure characterisation, propofol was administered intravenously at 15 mg/kg (National Veterinary Services Ltd., Stoke-on-Trent, UK) to each of the six animals in which seizures were successfully induced. The effect of propofol on seizure induction was then determined by electrically stimulating the sensorimotor cortex or perforant path at regular intervals, in accordance with the developed neocortical and hippocampal epileptic AD models. Electrophysiological recordings were monitored to determine the presence or absence of seizures following each stimulation. Once seizure activity returned in the EEG traces and seizures could be induced reliably, a second dose of propofol was administered at 15 mg/kg and electrical stimulation with the optimised parameters was repeated to confirm the effects of the drug on seizure induction. This process was repeated once more, resulting in a total of three intravenous doses of propofol over several hours in each animal.

2.6. ECoG and LFP data acquisition

ECoG and LFP recordings were made from all available epicortical and depth electrodes with respect to a reference electrode, comprising a Ag-AgCl plate that was 9 mm in diameter, placed beneath the nuchal skin. Voltage changes recorded from the cortical surface and hippocampus were digitised at a sampling frequency of 25 kHz using the actiCHamp 128-channel EEG amplifier (Brain Products GmbH, Gilching, Germany) and data acquisition was controlled using the BrainVision Recorder software (Brain Vision LLC, Morrisville, NC, USA). LFP data collected by the 16 depth electrode contacts were passed through a unity gain headstage amplifier (HST/32o25-GEN3-36P-G1; Plexon, Dallas, TX, USA) prior to reaching the EEG amplifier. At least 30 s of baseline EEG activity was recorded prior to each stimulation and a further 60-80 s of activity was recorded after the end of stimulation to determine whether epileptic seizures had been successfully elicited. A 50-Hz notch filter (second order, IIR) for removal of mains noise, a 1 Hz high-pass filter (first order, Butterworth) and a 1 kHz low-pass filter (fifth order, Butterworth) were applied to the ECoG/LFP display.

2.7. Statistical analysis

The criteria for seizure detection were the sudden appearance of abnormal electrographic activity comprising a series of rhythmic and repetitive discharges with high amplitude (>2 times that of the baseline activity) and a minimum duration of 10 s (Abend & Wusthoff, 2012; Fisher, et al., 2014). To determine whether the success rates of seizure induction in rats anaesthetised with α-chloralose and fentanyl in the neocortical epileptic AD model were significantly different, Fisher's exact test was conducted. This statistical test is commonly used for the assessment of statistically significant differences between binary variables (in this case, the presence or absence of seizures in the ECoG display following cortical stimulation). For the hippocampal epileptic AD model, Fisher's exact test was used to assess whether the seizure induction rates differed significantly between the two stimulation protocols tested. In addition, a paired t-test was used to identify statistically significant differences in the duration of seizures induced by these two protocols. The order in which the two protocols were tested was randomised to eliminate potential carryover effects associated with either protocol, thereby confirming that any electrographic activity observed following stimulation was indeed due to the parameters used for seizure induction. This was further validated by providing sufficient time between the application of stimulus trains (≥7 min) for restoration of the resting brain activity, in accordance with the minimum inter-train interval required to prevent kindling of neural circuits due to repeated stimulation (Nelson, et al., 2010). For both the neocortical and hippocampal models, a one-way repeated

measures analysis of variance (ANOVA) test was conducted to confirm that the duration of seizures induced by a given combination of stimulation parameters did not differ significantly across stimulation attempts and animals. A significance level of $\alpha = 0.05$ was used for all statistical analyses. All data are presented as mean ± SD.

3. Results

3.1. Cortical stimulation in rats anaesthetised with fentanyl-isoflurane, but not α-chloralose, results in reliable seizure induction

Seven rats were required in total to obtain a working model of reproducible neocortical seizures in the anaesthetised rat. Under intravenous α-chloralose anaesthesia, electrical stimulation of the sensorimotor cortex with parameters in the ranges tested did not induce epileptiform discharges (N = 4 rats); the overall success rate for the induction of seizures was 0% of 107 attempts across the four animals (Fig. 4). In these rats, baseline cortical activity observed in the ECoG recording comprised hypersynchronous delta waves, 200-800 μV in amplitude and <250 ms in duration at a frequency of 1-2 Hz (Fig. 5a). Stimulation of the sensorimotor cortex consistently induced an abrupt, generalised suppression of this resting activity. The duration of this suppression phenomenon increased with escalating stimulus intensities; however, no epileptiform discharges could be elicited despite varying the pulse waveform, pulse width, amplitude, frequency, duration and inter-train interval of stimulation.

In contrast, seizures were reliably induced in animals anaesthetised with a combination of intravenously administered fentanyl and ~0.5% isoflurane (N = 3 rats). The first protocol tested in these rats, which involved stimulation of the sensorimotor cortex with a 10-s train of biphasic symmetric, charge-balanced square-wave pulses (pulse width: 1 ms; amplitude: 1 mA) delivered at 100 Hz, successfully elicited neocortical seizures which had a focus within the facial region of the primary somatosensory cortex. The stimulation parameters were further optimised to minimise the current delivered to the brain whilst maintaining the stereotypic pattern of epileptiform discharges. The final developed model involved stimulating the sensorimotor cortex with a 5-s train of biphasic symmetric, charge-balanced square-wave pulses, 1 ms in pulse width, delivered at 100 Hz. As expected, the current threshold for induction of ictal discharges was variable across rats and lay in the 1.5-2 mA range (1.7 ± 0.3 mA; N = 3 rats). 14 stimulation attempts with these optimised parameters were performed in each of the three animals. The percentage of attempts that resulted in seizure induction in the three rats were 92.9% (13/14), 100% (14/14) and 92.9% (13/14), respectively. The overall success rate for the induction of seizures across all animals was 95.2% of a total of 42 attempts (Fig. 4a).

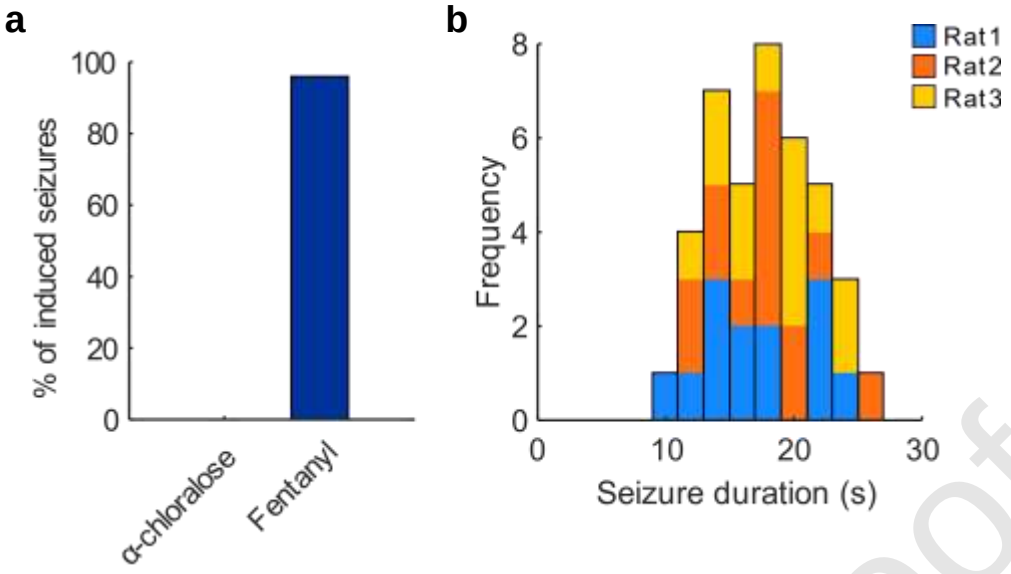

Figure 4. Development of neocortical epileptic AD model. (**a**) Bar chart displaying the percentage of seizures induced out of total stimulation attempts for the two anaesthetics tested. The overall success rates for seizure induction across all animals under α-chloralose and fentanyl-isoflurane anaesthesia were 0% (0/107 attempts, $N = 3$ rats) and 95.2% (40/42 attempts, $N = 3$ rats), respectively, and were thus significantly different ($p < 0.05$, Fisher's exact test). (**b**) Histogram of seizure duration for seizures induced by the optimised cortical stimulation protocol in the three rats anaesthetised with fentanyl-isoflurane (bin width: 2 s). The seizures for each animal are represented in a different colour.

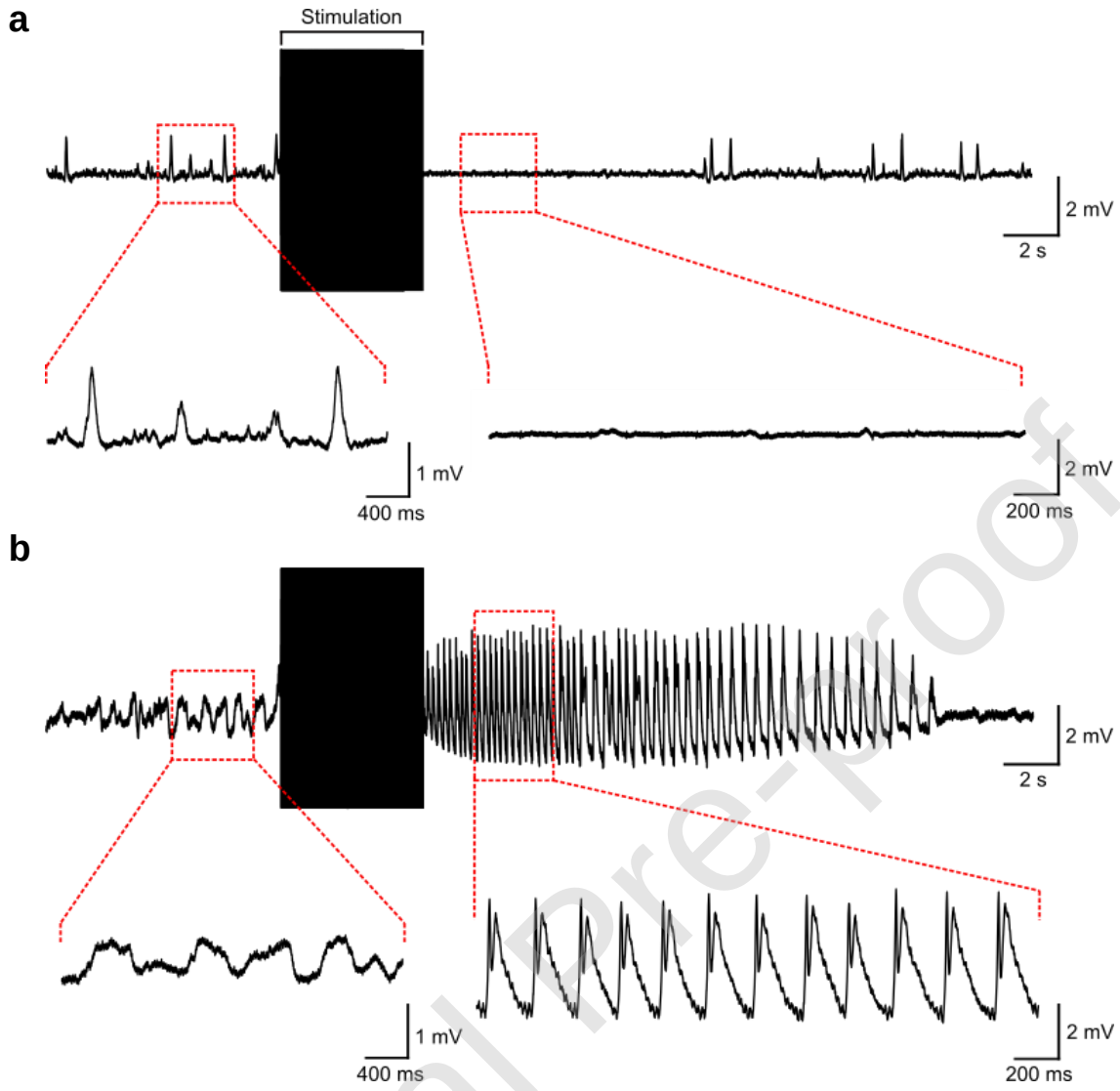

Figure 5. Representative ECoG recordings displaying the electrographic effects of electrically stimulating the sensorimotor cortex of rats under α-chloralose and fentanyl-isoflurane anaesthesia. Stimulation series comprised a 5-s train of biphasic symmetric square-wave pulses (pulse width: 1 ms; amplitude: 1.5 mA) at 100 Hz. (**a**) In rats anaesthetised with α-chloralose, a temporary suppression of the baseline delta rhythm, which consisted of hypersynchronous high-amplitude delta waves, was observed following electrical stimulation; however, epileptiform discharges could not be elicited. (**b**) Under fentanyl-isoflurane anaesthesia, cortical stimulation with the same parameters consistently induced ictal events comprising a series of repeatable SWDs at 2-5 Hz. The differences in the resting state of the brain between the two anaesthetics, evidenced by sharp (**a**) versus slow (**b**) delta waves, may explain these contrasting abilities to present ictal activity in response to electrical stimulation. Both ECoG traces were recorded by the same electrode within the 57-eletrode epicortical array on the rat brain, which lay above the facial representation within the primary somatosensory cortex and corresponded to the ictal focus in (**b**).

3.2. Characterisation of seizures induced by the neocortical epileptic AD model

Neocortical seizures consisted of a stereotypic pattern of focal, rhythmic spike-and-wave discharges (SWDs) at 2-5 Hz, and minimum peak-to-peak amplitude of 2 mV, which occurred immediately after the end of stimulation (Fig. 5b), occasionally followed by more variable epileptic discharges including sharp waves and polyspike-and-wave complexes. The ictal events induced by the optimised combination of stimulus parameters had a mean duration of 17.7 ± 3.8 s across all animals anaesthetised with fentanyl-isoflurane (Fig. 4b; n = 40 seizures, N = 3 rats). The mean seizure duration in each rat was 18.3 ± 3.7 s, 17.1 ± 4.0 s and 17.6 ± 3.7 s, respectively. The seizure duration did not differ significantly across stimulation attempts and between animals ($p > 0.05$, one-way repeated measures ANOVA). Across seizures and animals, the ictal focus was consistently recorded from the same electrode on the epicortical array which lay above the facial region of the primary somatosensory cortex. An inter-train interval of ≥7 min was necessary to allow the resting baseline ECoG rhythm, which comprised slower delta waves (>400 ms in duration) than in α-chloralose-anaesthetised rats, to be restored following a post-ictal period of electrical quiescence. This interval ensured that the electrographic patterns of epileptiform discharges remained consistent over time. Motor manifestations of seizures were also observed: tonic posturing occurred during the cortical stimulation period and the ictal events themselves were accompanied by facial and contralateral forelimb clonus at a frequency matched to that of the ictal discharges.

3.3. Perforant path stimulation in rats anaesthetised with fentanyl-isoflurane results in reliable seizure induction

Since the anaesthetic combination and stimulus parameters most permissive for the induction of ictal discharges had been established during development of the neocortical epileptic AD model, fewer rats were required to develop a model of repeatable hippocampal epileptiform activity in the anaesthetised rat. Electrical stimulation of the perforant path projection with both stimulation protocols tested, which differed in pulse width and train duration, successfully elicited ictal events in the hippocampus under fentanyl-isoflurane anaesthesia (N = 3 rats). In each rat, 15 seizures were induced in total: 6 seizures were induced using stimulation protocol 1 and 9 seizures were induced using stimulation protocol 2. For protocol 1, the percentage of attempts that resulted in seizure induction in the three animals were 100% (6/6), 85.7% (6/7) and 85.7% (6/7), respectively. For protocol 2, the percentage of attempts that resulted in seizure induction in the three animals were 100% (9/9), 100% (9/9) and 90% (9/10), respectively. The overall success rates for the induction of seizures across all animals was 90.0% of a total of 20 attempts for protocol 1 and 96.4% of a total of 28 attempts for protocol 2 (Fig. 6a).

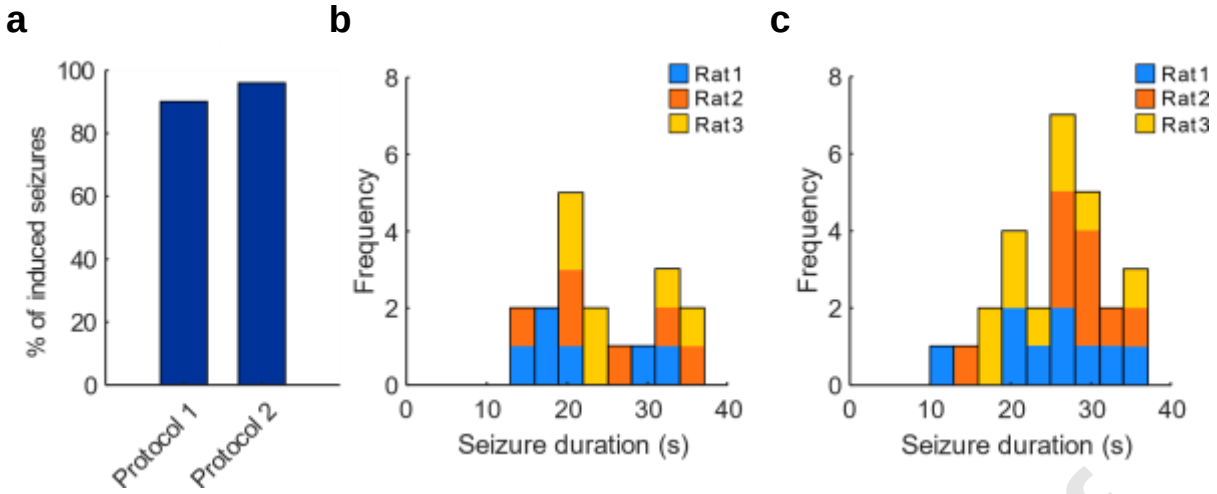

Figure 6. Development of hippocampal epileptic AD model. (**a**) Bar chart displaying the percentage of seizures induced out of total stimulation attempts with the two stimulation protocols tested under fentanyl-isoflurane anaesthesia. The overall success rates for seizure induction across all animals for protocols 1 and 2 were 90% (18/20 attempts, N = 3 rats) and 96.4% (27/28 attempts, N = 3 rats), respectively, and did not differ significantly ($p > 0.05$, Fisher's exact test). Histograms of seizure duration for seizures induced by protocol 1 (**b**) and protocol 2 (**c**) in the three rats (bin width: 3 s). The seizures for each animal are represented in a different colour. There were no significant differences in seizure duration between the two protocols ($p > 0.05$, paired t-test).

3.4. Characterisation of seizures induced by the hippocampal epileptic AD model

The induced seizures comprised repeatable series of focal high-amplitude (2-15 mV) rhythmic granule cell population spikes, 30-50 Hz in frequency, recorded from the dentate granule cell layer (Fig. 7). The ictal focus, defined as the position of the recording electrode on the 16-channel LFP probe from which the highest-amplitude population spikes were recorded, remained consistent across seizures in each animal. No discernible activity that met the requirements for seizure detection could be observed on the epicortical electrodes, confirming that the ictal spikes indeed originated in local microcircuits within the dentate gyrus. The mean duration of seizures induced by stimulation protocols 1 and 2 across all animals were, respectively, 24.4 ± 6.8 (n = 18 seizures, N = 3 rats) and 26.3 ± 6.5 s (n = 27 seizures, N = 3 rats) and did not differ significantly between the two protocols (Fig. 6; $p > 0.05$, paired t-test). For protocol 1, the mean seizure duration in each of the three rats was 25.8 ± 6.5 s, 24.9 ± 6.8 s and 22.6 ± 6.6 s, respectively. For protocol 2, the mean seizure duration in each rat was 24.6 ± 5.7 s, 28.3 ± 6.6 s and 25.9 ± 6.5 s, respectively. The duration of seizures induced by both of the stimulation protocols tested did not differ significantly across stimulation attempts and between rats ($p > 0.05$, one-way repeated measures ANOVA). The effects of electrical stimulation with a given set of parameters were therefore shown to be consistent and reproducible within and across animals.

Stimulation protocol 2, in which the angular bundle of the perforant path was stimulated with a 2-s train of biphasic symmetric, charge-balanced square-wave pulses (pulse width: 1 ms) at 100 Hz, was chosen for the final adapted model. This is because the first ictal discharges induced by this protocol consistently occurred after the end of the 2-s stimulation period, enabling clear visualisation of the seizure onset in the LFP recordings (Fig. 7b), in contrast to the initial ictal discharges generated by protocol 1 which occurred during the 5-s stimulus train (Fig. 7a). Additionally, use of protocol 2 minimised the overall current delivered to the perforant path to induce repeatable seizures. Using the chosen combination of stimulus parameters, discrete hippocampal ictal events could be induced

consistently at a current amplitude of 1.5 mA. An inter-train interval of ≥12 min was required to ensure that seizures remained electrographically reproducible. The stimulation parameters and seizure properties for the neocortical and hippocampal epileptic AD model are summarised (Table 2).

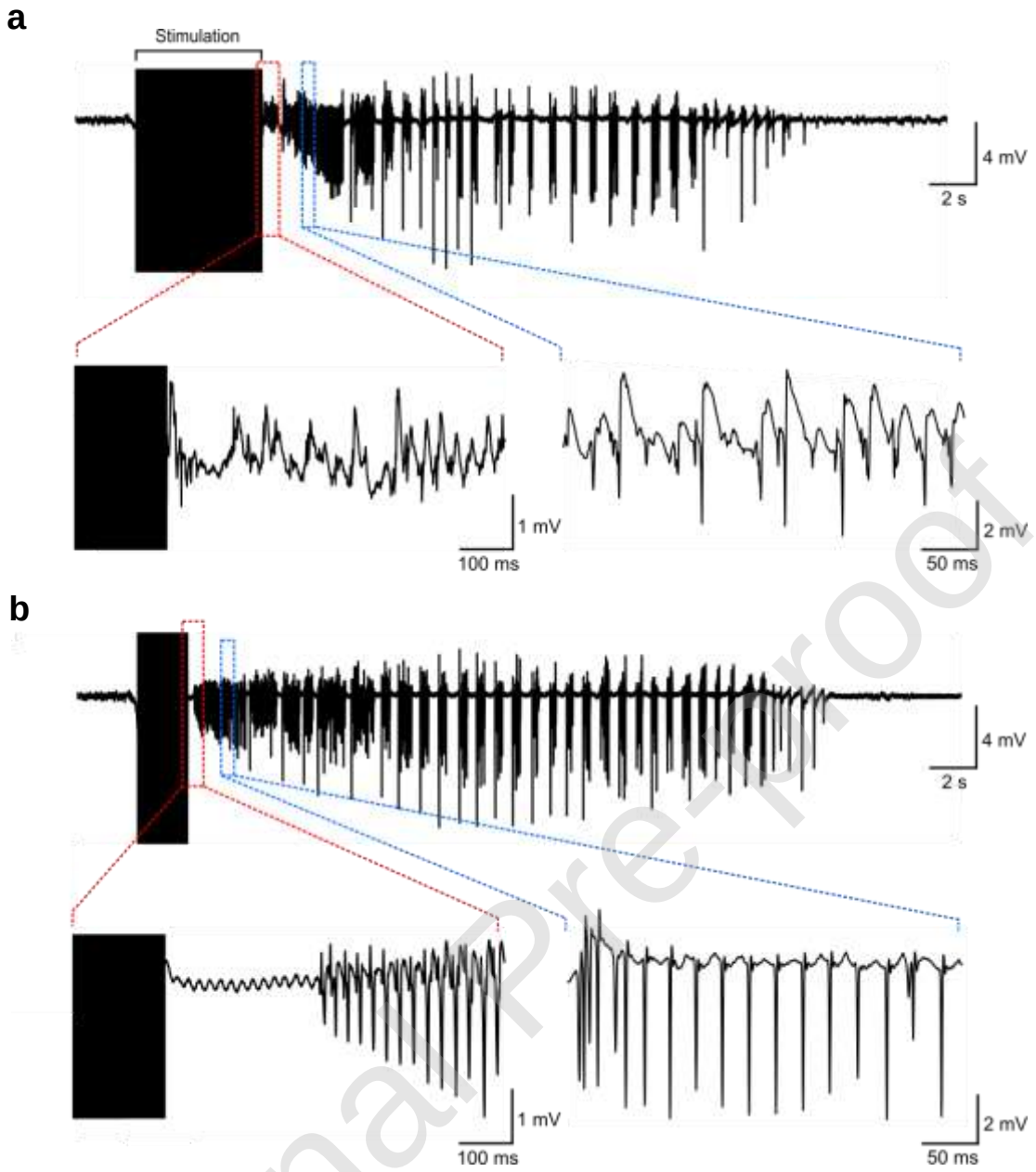

Figure 7. Representative LFP recordings displaying the electrographic effects of electrically stimulating the perforant path of rats under fentanyl-isoflurane anaesthesia with two stimulation protocols. Stimulation with: (**a**) a 5-s train of biphasic symmetric, charge-balanced square-wave pulses with a pulse width of 0.1 ms (protocol 1), and (**b**) a 2-s train of biphasic square-wave pulses with a pulse width of 1 ms (protocol 2), both delivered at 100 Hz and 1.5 mA, consistently induced hippocampal ictal events comprising bursts of high-amplitude population spikes, sometimes superimposed on field EPSPs. In contrast to protocol 1 (**a**), the initial discharges in seizures elicited by protocol 2 (**b**) occurred after the end of the 2-s stimulation period following a brief pre-ictal period of >200 ms and so were not contaminated by electrical stimulation artefacts in the LFP recordings. Additionally, the induced seizures comprised ictal paroxysmal discharges which were more repeatable than those elicited by protocol 1. For these reasons, protocol 2 was selected for the adapted model. Both LFP traces were recorded from the ninth most dorsal electrode on the 16-channel linear depth probe, corresponding to the ictal focus within the granule cell layer of the dentate gyrus.

Model	Stimulation parameters							Seizure properties	
	Site	Pulse waveform	Pulse width (ms)	Frequency (Hz)	Train duration (s)	Amplitude (mA)	Inter-train interval (min)	Electrographic features	Duration (s)
Neocortical epileptic AD model	Sensorimotor cortex	Biphasic symmetric, charge-balanced square-wave pulses	1	100	5	1.5-2	7	Rhythmic series of focal SWDs, ≥2 mV in amplitude, at 2-5 Hz; observed immediately after end of stimulating period; occasionally followed by sharp waves	17.7 ± 3.8
Hippocampal epileptic AD model	Angular bundle of perforant path	Biphasic symmetric, charge-balanced square-wave pulses	1	100	2	1.5	12	Rhythmic series of focal granule cell population spikes, 2-15 mV in amplitude, at 30-50 Hz; observed following >200 ms electrically quiescent period at the end of stimulating period	26.3 ± 6.5

Table 2. Summary of optimised stimulation protocols and seizure properties for the neocortical and hippocampal epileptic AD models. For both models, all stimulation series were delivered to rats anaesthetised with a combination of isoflurane (~0.5 %) and intravenously administered fentanyl (20 μg/kg/h). The fact that the hippocampus consistently generated longer-lasting series of epileptiform discharges, despite receiving a shorter stimulation train (2 s) than the sensorimotor cortex in the neocortical model (5 s), illustrates its high susceptibility to neuronal hypersynchrony.

3.5. Propofol prevents induction of neocortical and hippocampal seizures with electrical stimulation

The effect of propofol, which has established antiseizure properties, on the optimised neocortical and hippocampal epileptic AD models was assessed to confirm their clinical responsiveness. For both models, propofol was administered intravenously and the sensorimotor cortex or perforant path was periodically stimulated to determine whether seizures could be induced. Electrical stimulation was performed every 7 and 12 minutes for the neocortical and hippocampal epileptic AD models, respectively, since these were the minimum inter-train intervals that enable resting baseline EEG activity to be restored after stimulation, as determined during model development. After propofol administration, neocortical or hippocampal epileptiform discharges could not be induced in any of the animals tested by electrical stimulation with the optimised parameters (Fig. 8). For the neocortical epileptic AD model, the mean time taken across all animals for seizures with the expected electrographic characteristics (see section 3.2) to be observed in the ECoG recordings was 29.0 ± 2.9 min after administering propofol (Fig. 8a; n = 9 doses, N = 3 rats). The mean recovery time for neocortical seizures across the three propofol doses in each rat was 28.0 ± 2.2 min, 28.7 ± 4.0 and 30.3 ± 1.2, respectively. For the hippocampal epileptic AD model, the mean time taken across all animals for seizures representative of this model (see section 3.4) to return in the LFP recordings from the dentate gyrus was 40.0 ± 3.3 min after the propofol dose (Fig. 8b; n = 9 doses, N = 3 rats). The mean recovery time for hippocampal seizures across the three propofol doses in each rat was 38.3 ± 1.2 min, 42.7 ± 4.5 and 39.0 ± 0.8, respectively.

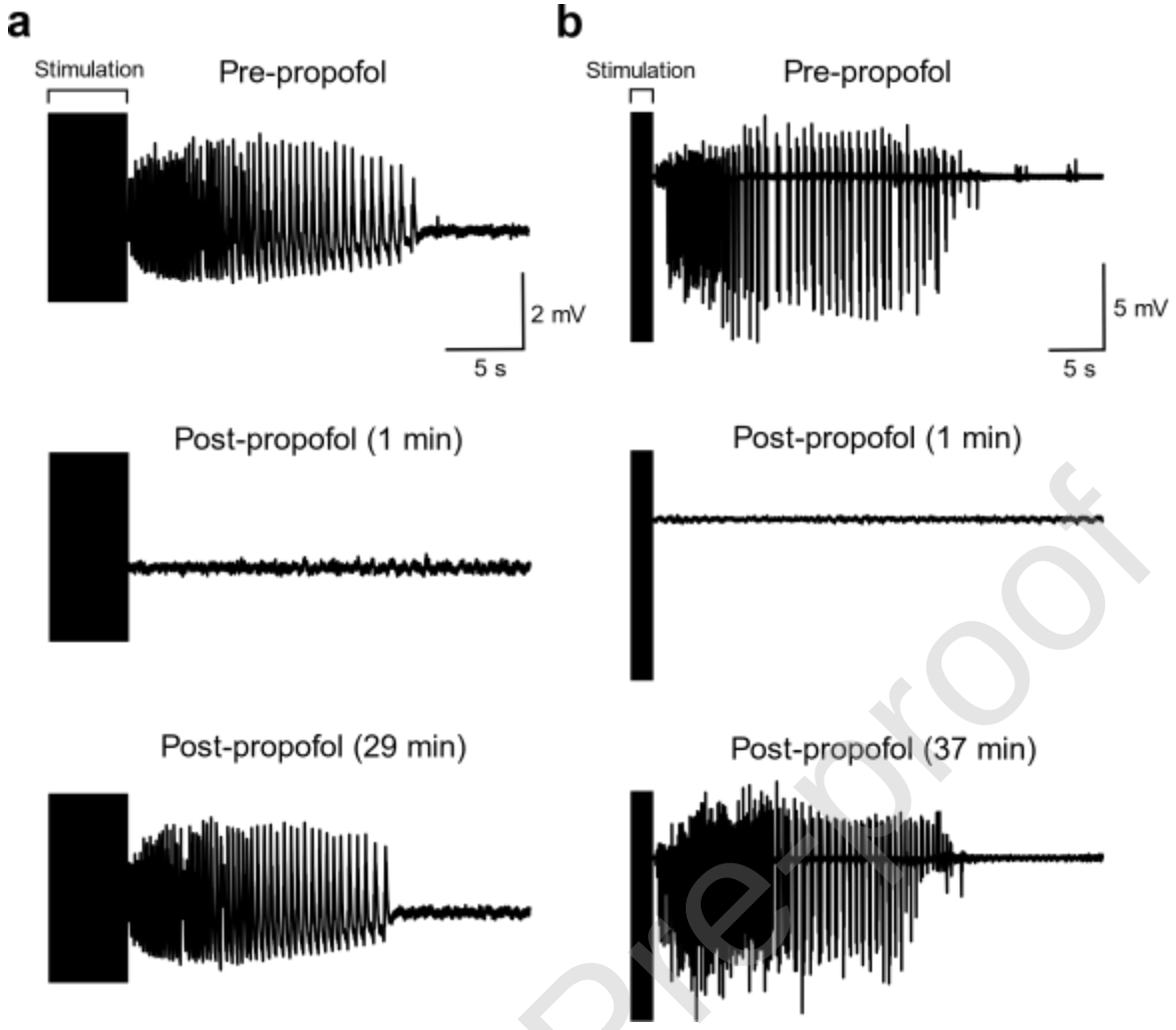

Figure 8. Representative EEG recordings displaying the effects of propofol on the ability to induce neocortical and hippocampal seizures with electrical stimulation. (**a**) ECoG traces, recorded from the ictal focus in the facial representation of the primary somatosensory cortex, show that administration of propofol (15 mg/kg, i.v.) immediately prevents the induction of seizures using the optimised electrical stimulation parameters for the neocortical epileptic AD model. (**b**) A similar response was seen for the hippocampal epileptic AD model; LFP traces recorded from the ictal focus within the dentate granule cell layer displayed an inability to induce hippocampal seizures with the optimised stimulation parameters following propofol administration. Electrical stimulation was performed at intervals of 7 and 12 min for the neocortical and hippocampal models, respectively, in accordance with the optimised minimum inter-train intervals. In these examples, neocortical and hippocampal seizures with the expected electrographic characteristics of the developed models could not be induced until 29 and 37 min, corresponding to the fifth and fourth stimulation attempts, after administering the propofol dose. ECoG recordings (**a**) were obtained using an electrode on the 57-electrode epicortical array and LFP recordings (**b**) were obtained using the ninth most dorsal electrode on the 16-channel linear depth probe, positioned at the respective ictal foci for the induced neocortical and hippocampal seizures.

4. Discussion

In this study, we have developed and characterised two acute *in vivo* models of focal seizures, the neocortical and hippocampal epileptic AD models, for inducing stereotypic ictal epileptiform activity respectively in the neocortex and hippocampus of the generally anaesthetised rat. The optimised electrical stimulation parameters enabled the induction of reproducible, self-sustaining ictal events, localised to a well-defined focal origin in the neocortex or hippocampus, on demand under fentanyl-isoflurane anaesthesia. The seizures elicited comprised trains of electrographically repeatable ictal discharges which occurred immediately after delivery of the stimulus train. As such, the timing of these events can be tightly regulated, rendering the adapted models an efficient and well-tolerated means for the screening of novel anticonvulsant therapies and suitable for studies investigating the mechanisms of epileptogenesis that require complete control of seizure timing in the anaesthetised state.

4.1. Effects of anaesthetic agents on seizure induction

The choice of agent for maintaining general anaesthesia during the induction of ictal events was an important consideration and was expected to require some method development as the electrical AD models of epilepsy are typically used in awake rats (Kubová, et al., 1996; Bragin, et al., 1997; Krupp & Löscher, 1998; Velísek & Mares, 2004; Nelson, et al., 2010; Fábera & Mares, 2014). During development of the neocortical epileptic AD model, epileptiform discharges could not be induced by electrical stimulation of the sensorimotor cortex in rats anaesthetised with α-chloralose despite increasing the current amplitude of the delivered stimulus to 15 mA and testing a range of pulse waveforms, pulse widths, frequencies, train durations and inter-train intervals. Limited *in vitro* studies have suggested that α-chloralose induces anaesthesia by increasing the affinity of $GABA_A$ receptors for the inhibitory neurotransmitter GABA through allosteric modulation of the GABA binding site, which thus potentiates $GABA_A$ receptor-induced inhibitory currents (Kumamoto & Murata, 1996; Garrett & Gan, 1998). It is known to have dose-dependent effects, both excitatory and inhibitory, on the CNS (Winters & Spooner, 1966; Segev, et al., 2006). A documented feature of α-chloralose is its ability to induce generalised inhibition which leads to synchronisation of cortical activity, giving rise to ECoG recordings characterised by intermittent high-amplitude transients (Winters & Spooner, 1966; Peeters, et al., 2001). This phenomenon was consistently observed in the present study; sharp hypersynchronous delta waves, >200 μV in amplitude and <250 ms in duration, were visible in the baseline ECoG recording at a frequency of 1-2 Hz shortly after introducing α-chloralose (Fig. 5a). In contrast, Rao demonstrated the presence of a low-voltage, electrically quiescent baseline ECoG prior to stimulus application to the rabbit cortex in one of the only acute studies reporting the successful use of this epilepsy model under α-chloralose anaesthesia (Rao, 2000). Therefore, the presence of hypersynchronous delta waves in the present study, which may be indicative of generalised cortical inhibition (Segev, et al., 2006), is the most probable explanation for the failure to elicit epileptiform discharges in our initial experiments. This is further supported by the inhibitory effects of propofol, which also enhances $GABA_A$ receptor-mediated inhibition (Weir, et al., 2017), on our seizure models.

In order to avoid this generalised inhibition, the intravenously administered dose of α-chloralose would have needed to be varied by assessing its effects on resting ECoG activity whilst ensuring maintenance of an areflexic state. The optimal dose would, however, be difficult to establish as α-chloralose has a relatively long plasma half-life of 8-10 hours in rats (Fish, et al., 2008). For this reason, we decided to first test fentanyl (with ~0.5% isoflurane) for its potential in this study. Because epileptiform discharges could be induced immediately with this anaesthetic combination, its use was continued for all subsequent experiments aimed at optimising stimulation parameters in both the neocortical and hippocampal epileptic AD models.

4.2. Characteristics of the adapted neocortical and hippocampal epileptic AD models

The developed neocortical and hippocampal epileptic AD models involve electrical stimulation of the sensorimotor cortex or perforant path, respectively, with trains of biphasic symmetric, charge-balanced square-wave pulses, 1 ms in pulse width and 1-2 mA in amplitude, at 100 Hz in rats anaesthetised with fentanyl-isoflurane. In the neocortical model, a 5-s train is delivered through two electrodes on a 57-electrode epicortical array either side of the boundary between the primary somatosensory and motor cortex (M1/S1 HL). In the hippocampal model, a 2-s train of the same stimulus pulses is applied through a twisted bipolar stimulating electrode targeting the perforant path projection from Layer II/III of the entorhinal cortex.

In this study, ictal activity was defined as repetitive epileptiform discharges lasting ≥10 s based on the majority of seizures recorded in humans (Jenssen, et al., 2006; Hughes, 2009; Cook, et al., 2016). The seizures induced by the optimised stimulation parameters were 17.7 ± 3.8 s and 26.3 ± 6.5 s for the neocortical and hippocampal models, respectively. Additionally, they were stereotypic and consistent in their electrographic manifestations: focal high-amplitude rhythmic paroxysms, with a frequency of 2-5 Hz for neocortical ictal discharges and 30-50 Hz for hippocampal ictal discharges, were generated immediately after the end of electrical stimulation. These features are in agreement with previous studies that have utilised epileptic AD models in freely moving rats (Leung, 1987; Bragin, et al., 1997; Haugvicová, et al., 2002; Nelson, et al., 2010; Fábera & Mares, 2014) and are also comparable to the electrographic patterns of spontaneous recurrent seizures induced by several chemical models of epilepsy, including the kainic acid (Cavalheiro, et al., 1982) and pilocarpine models (Leite, et al., 1990). In addition, the electrographic features of the induced epileptiform activity closely resemble those of acute seizures induced by administration of the chemoconvulsant 4-aminopyradine into the rat hippocampus and neocortex (Peña & Tapia, 2000; Bahar, et al., 2006). The ictal focus, as determined by recording electrodes, was consistently localised to the facial somatosensory cortex in the neocortical model and the granule cell layer of the dentate gyrus in the hippocampal model; the positions of seizure foci also remained extremely stable across seizures and animals. A minimum inter-train interval of 7 and 12 min is required, respectively, for the neocortical and hippocampal models to enable baseline EEG activity to return following electrical stimulation and thus ensure that the electrographic presentation of seizures remain stable over time. This stability of the generated seizures and ability to control their induction demonstrate the usefulness of these models for testing the efficacy of novel anticonvulsant therapies and *in vivo* investigations that are restricted to an acute experimental setup. Further, the administration of propofol, a clinically used anaesthetic agent with antiseizure properties, consistently resulted in the inability to induce neocortical or hippocampal seizures following electrical stimulation with the optimised parameters. The time taken for seizures to return following intravenous propofol administration (29.0 ± 2.9 min in the neocortical model and 40.0 ± 3.3 min in the hippocampal model) was in agreement with the relatively short half-life of the drug (Folino & Parks, 2020). This complete suppression of epileptiform activity by propofol demonstrates that the developed models are highly predictive of the clinical response to an established antiseizure anaesthetic, thus validating their use in the preclinical testing of novel treatments for seizures.

4.3. Potential applications for the adapted neocortical and hippocampal epileptic AD models

The major advantages of the epileptic AD models adapted for inducing neocortical and hippocampal seizures acutely in this study are as follows. First, these models enable ictal epileptiform events to be elicited on demand under anaesthetised conditions, immediately after the delivery of a stimulus comprising a train of square-wave pulses. This overcomes the technical challenges associated with the use of chronic models of spontaneous seizures in freely moving animals such as the need for prolonged

training of animals to habituate them to recording procedures and offline video EEG-monitoring to establish the efficacy of potential antiseizure treatments, which are laborious and time-consuming, and therefore largely simplifies the screening of novel therapeutic interventions for epilepsy (Blumenfeld, 2007). As such, the implementation of these models can provide an efficient method with which to test antiseizure drugs in early pre-clinical phases and evaluate potential stimulation paradigms for focal electrical stimulation, a promising therapeutic alternative for refractory epilepsies, with high throughput and reproducibility.

The ability of the neocortical and hippocampal epileptic AD models to induce seizures acutely with controlled and predictable timing is also a valuable feature for neuroimaging studies. Several functional imaging modalities including EIT, BOLD-fMRI and diffusion MRI require long-lasting sessions of recording in head-fixed animals, which are typically anaesthetised and paralysed to eliminate movement artefacts associated with extreme muscle activity during seizures, for the acquisition of adequate high-quality data and accurate image reconstruction (Nersesyan, et al., 2004; Blumenfeld, 2007; Airaksinen, et al., 2011; Tsurugizawa, et al., 2013; Hannan, et al., 2018a). For such applications, therefore, it is vital to be able to induce seizures reliably and reproducibly under anaesthetised and paralysed conditions to maximise data acquisition, which can be achieved by the presented models. By simplifying the experimental setup required for imaging functional changes during epileptiform events, implementation of the adapted epileptic AD models may also open the door to proof-of-concept studies of novel neuroimaging approaches and ultimately improve understanding of the altered functional connectivity in epileptogenic networks.

Secondly, the developed models represent focal models of neocortical and hippocampal epilepsy which can be used to test focal treatments. For example, they may be employed for assessing the efficacy of different stimulation parameters in closed-loop neuromodulation systems, which are competing alternatives to pharmaceutical anticonvulsants, for the treatment of refractory focal epilepsies (Fountas & Smith, 2007; Bigelow & Kouzani, 2019). The presence of a precisely defined ictal focus in the neocortical and hippocampal AD models is particularly advantageous for imaging studies in which reconstructions often need to be compared across animals to determine reproducibility and thus evaluate the technical accuracy of a given imaging modality. In addition, the sites of electrical stimulation are remote from the expected location of maximal activity due to strong functional connectivity between both (a) the sensorimotor and facial somatosensory cortical regions and (b) the entorhinal cortex and the dentate gyrus via the perforant path. This is beneficial for neuroimaging experiments where the presence of stimulating electrodes or microdialysis probes in close proximity to the ictal focus can result in reconstruction artefacts within the target region for imaging epileptiform activity. In particular, for EIT protocols, the presence of an implanted object near the ictal focus which has contrasting conductivity to the surrounding cerebral tissue can affect the current distribution during impedance measurements which would, in turn, influence the spatial sensitivity profile of the imaging protocol and therefore reduce the quality and localisation accuracy of reconstructions (Hannan, et al., 2020). The presented models thus avoid such effects on the resulting images and provide a method that enables inter-subject comparisons of reconstructed functional changes during epileptiform events.

Moreover, the injection of chemoconvulsants into the neocortex or hippocampus in chemical models of epilepsy may itself affect the measured signal during imaging protocols with BOLD-fMRI or EIT, for example, and thus lead to difficulties in establishing the true source of any imaged activity (Renvall, et al., 2014; Hannan, 2019). Inducing seizures with the presented neocortical and hippocampal epileptic AD models, on the other hand, avoids such fluid-related alterations in the BOLD or tissue impedance response, thereby validating that the images are truly reflective of neural activity during epileptiform events.

A limitation of this study was that only female rats were used to develop the neocortical and hippocampal epileptic AD models. However, our goal was to establish simple, practical and highly accessible models of seizures with stereotypic and reproducible electrographic features to use in acute setups under anaesthetised conditions. As such, investigating any potential effects of sex differences on these models lay outside the scope of the present work. Moreover, detailed protocols for localising the target brain regions for electrical stimulation, namely the sensorimotor cortex and the angular bundle of the perforant path for the neocortical and hippocampal models respectively, with high precision using functional mapping based on ECoG and LFP recordings are provided in our methods. This approach enables the precise stimulation location to be determined in each individual rat. Similarly, the current threshold required to elicit epileptiform discharges, which is expected to vary slightly across animals due to age and weight differences (Kubová, et al., 1996; Krupp & Löscher, 1998), is also determined per animal. Therefore, if these described protocols are followed to account for any inter-individual variabilities, it is expected that the optimised stimulation parameters will enable the generation of epileptiform events with similarly reproducible electrographic characteristics, despite any potential neuroanatomical or size differences across sexes. This is further supported by the fact that no sex differences in seizure properties were observed in previous studies that have used the electrical AD models of epilepsy in awake, freely moving rats (Bragin, et al., 1997; Langberg, et al., 2016). Nonetheless, future work can be done to explicitly investigate whether any differences exist between male and female animals when using the optimised models.

The neocortical and hippocampal epileptic AD models developed in the present study are also limited in their lack of cell-type specificity and thus inability to influence the firing characteristics of specific neuronal populations to induce seizures. The contribution of specific cell types to epileptiform activity may be determined by employing optogenetic approaches for seizure induction (Cela & Sjöström, 2019). Osawa et al. (2013) demonstrated that repetitive photostimulation of the rat hippocampus, in which channelrhodopsin-2 (ChR2) was expressed, reproducibly results in seizure-like afterdischarges. Similarly, a mouse model of optogenetic seizure induction in the neocortex, in combination with calcium imaging, was used to delineate the roles of different populations of interneurons in seizure initiation and maintaining ictal activity (Khoshkoo, et al., 2017). In addition, an optogenetic variant of the classical kindling model of epilepsy was developed in awake, freely moving mice by applying brief stimuli every two days to activate neocortical pyramidal cells (Cela, et al., 2019). This resulted in a progressive increase in the number and severity of seizures and elevated seizure susceptibility in the absence of additional stimulation (Cela, et al., 2019). Other studies have also combined kindling with optogenetics in this manner to give rise to a gradual intensification of stimulus-induced seizures in mice over time (Wang, et al., 2017; Berglind, et al., 2018). Although such approaches can circumvent the limitation of electrical stimulation in identifying the specific neuronal networks responsible for focal epileptogenicity, establishing transgenic lines that express functionally relevant levels of optical actuators of neuronal activity through genetic manipulation can be laborious, costly and time-consuming (Zeng & Madisen, 2012). Moreover, rats offer several advantages over mice as a disease model for use in EIT experiments and other imaging studies aimed at investigating neural network dynamics in epilepsy due, for example, to their larger body size and thus ability to accommodate a greater number of electrodes (Anikeeva, et al., 2011). However, the limited number of established transgenic rat strains has hindered the application of optogenetics in rats (Igarashi, et al., 2018). Since we aimed to develop a simple and practical rat model of seizure induction for use in acute *in vivo* experimental setups, primarily for imaging neural activity during epileptiform events at the mesoscopic scale, utilising optogenetic tools to elucidate specific cell populations implicated in epileptogenesis was outside the scope of this study.

The main limitation of the adapted neocortical and hippocampal epileptic AD models relates to the fact that they are merely an approximation of a complex system that constitutes the human disease and the results should therefore be interpreted with caution, an inherent quality of all animal seizure models. There may also be specific differences between the mechanisms underlying such induced seizures compared to the spontaneous recurrent seizures that occur in human epilepsies (Gu & Daltone, 2017). Nevertheless, models of acute seizures have been shown to provide valuable information regarding the pharmacological profile of anticonvulsant drugs and can be especially useful for optimising efficiency during the initial 'identification' phase of the preclinical Epilepsy Therapy Screening Program (ETSP) (Kehne, et al., 2017; Löscher, 2017). Chronic models of epilepsy that mirror the spontaneous nature of human seizures, and therefore offer a more 'realistic' clinical representation of the condition, can subsequently be implemented at the later 'differentiation' phase of the ETSP (Löscher, 2017). Overall, a fit-for-purpose paradigm should be employed, in which the animal model used in a given study is selected on the basis of the characteristics required to answer the specific research questions under investigation (Löscher, 2016).

4.4. Conclusion

In summary, two optimised experimental models of focal neocortical and hippocampal seizures are presented, for use in generally anaesthetised rats, which provide an efficient method for investigating the mechanisms of human epilepsies and evaluating novel therapeutic strategies. The described models enable the reliable on-demand generation of focal ictal events localised to a known position within the neocortex or dentate gyrus by electrical stimulation with a set of specified parameters. As such, they hold promise for any *in vivo* investigations that necessitate tight regulation of seizure timing, for example, in acute neuroimaging studies aimed at elucidating changes in functional connectivity during epileptogenesis, or in which recovery of animals from anaesthesia is not possible or practical. Furthermore, the high reproducibility in the electrographic presentation of induced neocortical and hippocampal seizures in these models has potential to increase the power of comparisons of novel treatments during preclinical screening and consequently reduce the total number of animals needed. Implementation of the presented models can, therefore, provide a cost-effective acute experimental setup with which to test anticonvulsant drugs and evaluate closed-loop stimulation paradigms for the treatment of refractory focal epilepsies, such as FNE and mTLE, with rapid throughput and a high degree of repeatability.

Author Contribution Statement

Sana Hannan: Conceptualisation, Data curation, Formal analysis, Investigation, Methodology, Visualisation, Writing – original draft preparation, Writing – reviewing and editing; **Mayo Faulkner:** Investigation, Methodology, Resources, Software; **Kirill Aristovich:** Formal analysis, Resources, Software; **James Avery:** Methodology, Software; **Matthew C. Walker:** Methodology; Supervision; Writing – reviewing and editing; **David S. Holder:** Conceptualisation, Funding acquisition, Supervision, Writing – reviewing and editing.

Declaration of competing interests

The authors declare that they have no conflicts of interest.

Acknowledgments

Funding: This work was supported by DARPA (grant number N66001-16-2-4066), Blackrock Microsystems and the EPSRC (grant number EP/M506448/1). James Avery was supported by the NIHR Imperial BRC.

References

Abend, N. S., & Wusthoff, C. J. (2012). Neonatal Seizures and Status Epilepticus. *J Clin Neurophysiol, 29*(5), 441-448.

Airaksinen, A. M., Niskanen, J.-P., Chamberlain, R., Huttunen, J. K., Nissinen, J., Garwood, M., . . . Gröhn, O. (2011). Simultaneous fMRI and local field potential measurements during epileptic seizures in medetomidine sedated rats using RASER pulse sequence. *Magn Reson Med, 64*(4), 1191-1199.

Anikeeva, P., Andalman, A. S., Witten, I., Warden, M., Goshen, I., Grosenick, L., . . . Deisseroth, K. (2011). Optetrode: A Multichannel Readout for Optogenetic Control in Freely Moving Mice. *Nat Neurosci, 15*(1), 163-170.

Aristovich, K. Y., Packham , B. C., Koo, H., dos Santos, G. S., McEvoy, A., & Holder, D. S. (2016). Imaging fast electrical activity in the brain with electrical impedance tomography. Neuroimage, 124(Pt A), 204-213.

Bahar, S., Suh, M., Zhao, M., & Schwartz, T. H. (2006). Intrinsic optical signal imaging of neocortical seizures: the 'epileptic dip'. *Neuroreport, 17*(5), 499-503.

Ben-Ari, Y. (1985). Limbic seizure and brain damage produced by kainic acid: mechanisms and relevance to human temporal lobe epilepsy. *Neuroscience, 14*(2), 375-403.

Berg, A. T., Berkovic, S. F., Brodie, M. J., Buchhalter, J., Cross, J. H., van Emde Boas, W., . . . Scheffer , I. E. (2010). Revised terminology and concepts for organization of seizures and epilepsies: report of the ILAE Commission on Classification and Terminology, 2005-2009. *Epilepsia, 51*(4), 676-685.

Berglind, F., Andersson, M., & Kokaia, M. (2018). Dynamic Interaction of Local and Transhemispheric Networks Is Necessary for Progressive Intensification of Hippocampal Seizures. *Sci Rep, 8*(1), 5669.

Bigelow, M. D., & Kouzani, A. Z. (2019). Neural stimulation systems for the control of refractory epilepsy: a review. *J Neuroeng Rehabil, 16*(1), 126.

Blair, R. D. (2012). Temporal Lobe Epilepsy Semiology. *Epilepsy Res Treat*, 751510.

Blumenfeld, H. (2007). Functional MRI studies of animal models in epilepsy. *Epilepsia, 48*(Suppl 4), 18-26.

Bragin, A., Penttonen, M., & Buzsáki, G. (1997). Termination of epileptic afterdischarge in the hippocampus. *J Neurosci, 17*(7), 2567-2579.

Buzsàki, G., Bickford, R. G., Ryan, L. J., Young, S., Prohaska, O., Mandel, R. J., & Gage, F. H. (1989). Multisite recording of brain field potentials and unit activity in freely moving rats. *J Neurosci Methods, 28*(3), 209-217.

Cavalheiro, E. A., Riche, D. A., & Le Gal La Salle, G. (1982). Long-term effects of intrahippocampal kainic acid injection in rats: a method for inducing spontaneous recurrent seizures. *Electroencephalogr Clin Neurophysiol, 53*(6), 581-589.

Cela, E., & Sjöström, P. J. (2019). Novel Optogenetic Approaches in Epilepsy Research. *Front Neurosci, 13*, 947.

Cela, E., McFarlan, A. R., Chung, A. J., Wang, T., Chierzi, S., Murai, K. K., & Sjöström, P. J. (2019). An Optogenetic Kindling Model of Neocortical Epilepsy. *Sci Rep, 9*, 5236.

Cendes, F. (2005). Mesial temporal lobe epilepsy syndrome: an updated overview. *J Epilepsy Clin Neurophysiol, 11*(3), 141-144.

Cook, M. J., Karoly, P. J., Freestone, D. R., Himes, D., Leyde, K., Berkovic, S., . . . Boston, R. (2016). Human focal seizures are characterized by populations of fixed duration and interval. *Epilepsia, 57*(3), 359-368.

Cross, D. J., & Cavazos, J. E. (2009). Circuitry Reorganization, Regeneration, and Sprouting. In P. A. Schwartzkroin (Ed.), *Encyclopedia of Basic Epilepsy Research* (pp. 1148-1154). Davis, CA: Elsevier Ltd.

Curia, G., Longo, D., Biagini, G., Jones, R. S., & Avoli, M. (2008). The pilocarpine model of temporal lobe epilepsy. *J Neurosci Methods, 172*(2-4), 143-157.

Fábera, P., & Mares, P. (2014). Effect of GABA(B) receptor agonist SKF97541 on cortical and hippocampal epileptic afterdischarges. *Physiol Res, 63*(4), 529-534.

Faulkner, M., Hannan, S., Aristovich, J., Avery, J., & Holder, D. (2018a). Characterising the frequency response of impedance changes during. *Physiol Meas, 39*(3), 034007.

Faulkner, M., Hannan, S., Aristovich, K., Avery, J., & Holder, D. (2018b). Feasibility of imaging evoked activity throughout the rat brain using electrical impedance tomography. *NeuroImage, 178*, 1-10.

Fish, R. E., Brown, M. J., Danneman, P. J., & Karas, A. Z. (2008). *Anesthesia and analgesia in laboratory animals* (2nd ed.). London: Academic Press.

Fisher, R. S., Scharfman, H. E., & deCurtis, M. (2014). How can we identify ictal and interictal abnormal activity? *Adv Exp Med Biol, 813*, 3-23.

Flecknell, P. (2015). *Laboratory animal anaesthesia* (4th ed.). London: Academic Press.

Folino, T. B., & Parks, L. J. (2020). *Propofol.* Treasure Island (FL): StatPearls Publishing.

Fountas, K. N., & Smith, J. R. (2007). A novel closed-loop stimulation system in the control of focal, medically refractory epilepsy. *Acta Neurochir Suppl, 97*(Pt 2), 357-362.

Garrett, K. M., & Gan, J. (1998). Enhancement of gamma-aminobutyric acid A receptor activity by alpha-chloralose. *J Pharmacol Exp Ther, 285*(2), 680-686.

Gu, B., & Daltone, K. A. (2017). Models and detection of spontaneous recurrent seizures in laboratory rodents. *Zool Res, 38*(4), 171-179.

Hannan, S. (2019). *Imaging fast neural activity in the brain during epilepsy with electrical impedance tomography.* PhD thesis: University College London.

Hannan, S., Faulkner, M., Aristovich, K., Avery, J., Walker, M. C., & Holder, D. (2018a). Imaging fast electrical activity in the brain during ictal epileptiform discharges with electrical impedance tomography. *Neuroimage Clin, 20*, 674-684.

Hannan, S., Faulkner, M., Aristovich, K., Avery, J., & Holder, D. (2018b). Frequency-dependent characterisation of impedance changes during epileptiform activity in a rat model of epilepsy. *Physiol Meas., 39*(8), 095003.

Hannan, S., Faulkner, M., Aristovich, K., Avery, J., & Holder, D. (2019). Investigating the safety of fast neural electrical impedance tomography in the rat brain. *Physiol Meas, 40*(3), 034003.

Hannan, S., Faulkner, M., Aristovich, K., Avery, J., Walker, M. C., & Holder, D. S. (2020). In vivo imaging of deep neural activity from the cortical surface during hippocampal epileptiform events in the rat brain using electrical impedance tomography. *Neuroimage, 209*, 116525.

Haugvicová, R., Bílková, E., Kubová, H., & Mares, P. (2002). Effects of classical antiepileptics on thresholds for phenomena induced by cortical stimulation in rats. *J Pharm Pharmacol, 54*(7), 1011-1015.

Hennessy, M. J., Elwes, R. D., Binnie, C. D., & Polkey, C. E. (2000). Failed surgery for epilepsy. A study of persistence and recurrence of seizures following temporal resection. *Brain, 123*(Pt 12), 2445-2466.

Hughes, J. R. (2009). Absence seizures: a review of recent reports with new concepts. *Epilepsy Behav, 15*(4), 404-412.

Hunfeld, M., Pope, K. J., Fitzgibbon, S. P., Willoughby, J. O., & Broberg, M. (2013). Effects of anesthetic agents on seizure-induction with intra-cortical injection of convulsants. *Epilepsy Res, 105*(1-2), 52-61.

Igarashi, H., Ikeda, K., Onimaru, H., Kaneko, R., Koizumi, K., Beppu, K., . . . Yawo, H. (2018). Targeted expression of step-function opsins in transgenic rats for optogenetic studies. *Sci Rep, 8*, 5435.

Jenssen, S., Gracely, E. J., & Sperling, M. R. (2006). How long do most seizures last? A systematic comparison of seizures recorded in the epilepsy monitoring unit. *Epilepsia, 47*(9), 1499-1503.

Kandratavicius, L., Balista, P. A., Lopes-Aguiar, C., Ruggiero, R. N., Umeoka, E. H., Garcia-Cairasco, N., . . . Leite, J. P. (2014). Animal models of epilepsy: use and limitations. *Neuropsychiatr Dis Treat, 10*, 1693-1705.

Kehne, J. H., Klein, B. D., Raeissi, S., & Sharma, S. (2017). The National Institute of Neurological Disorders and Stroke (NINDS) Epilepsy Therapy Screening Program (ETSP). *Neurochem Res, 42*(7), 1894-1903.

Kenny, J. D., Westover, M. B., Ching, S., Brown, E. N., & Solt, K. (2014). Propofol and sevoflurane induce distinct burst suppression patterns in rats. *Front Syst Neurosci, 8*, 237.

Khoshkhoo, S., Vogt, D., & Sohal, V. S. (2017). Dynamic, Cell-Type-Specific Roles for GABAergic Interneurons in a Mouse Model of Optogenetically Inducible Seizures. *Neuron, 93*(2), 291-298.

Kowski, A. B., & Holtkamp, M. (2015). Electrically Induced Limbic Seizures: Preliminary Findings in a Rodent Model. *J Exp Neurosci, 9*, 7-14.

Krupp, E., & Löscher, W. (1998). Anticonvulsant drug effects in the direct cortical ramp-stimulation model in rats: comparison with conventional seizure models. *J Pharmacol Exp Ther, 285*(3), 1137-1149.

Kubová, H., & Mares, P. (1995). Suppression of cortical epileptic afterdischarges by ketamine is not stable during ontogenesis in rats. *Pharmacol Biochem Behav, 52*(3), 489-492.

Kubová, H., Lanstiakova, M., Mockova, M., Mares, P., & Vorlicek, J. (1996). Pharmacology of cortical epileptic afterdischarges in rats. *Epilepsia, 37*(4), 336-341.

Kumamoto, E., & Murata, Y. (1996). Enhancement by lanthanide of general anesthetic-induced GABAA-receptor current in rat septal cholinergic neurons in culture. *J Neurophysiol, 75*(6), 2294-2299.

Langberg, T., Dashek, R., Mulvey, B., Miller, K. A., Osting, S., Stafstrom, C. E., & Sutula, T. P. (2016). Distinct behavioral phenotypes in novel "fast" kindling-susceptible and "slow" kindling-resistant rat strains selected by stimulation of the hippocampal perforant path. *Neurobiol Dis, 85*, 122-129.

Leite, J. P., Bortolotto, Z. A., & Cavalheiro, E. A. (1990). Spontaneous recurrent seizures in rats: an experimental model of partial epilepsy. *Neurosci Biobehav Rev, 14*(4), 511-517.

Leung, L. W. (1987). Hippocampal electrical activity following local tetanization. I. Afterdischarges. *Brain Res, 419*(1-2), 173-187.

Lhatoo, S. D., Solomon, J. K., McEvoy, A. W., Kitchen, N. D., Shorvon, S. D., & Sander, J. W. (2003). A prospective study of the requirement for and the provision of epilepsy surgery in the United Kingdom. *Epilepsia, 44*(5), 676-676.

Löscher, W. (2016). Fit for purpose application of currently existing animal models in the discovery of novel epilepsy therapies. *Epilepsy Res, 126*, 157-184.

Löscher, W. (2017). Animal Models of Seizures and Epilepsy: Past, Present, and Future Role for the Discovery of Antiseizure Drugs. *Neurochem Res, 42*(7), 1873-1888.

Luckl, J., Keating, J., & Greenberg, J. H. (2008). Alpha-chloralose is a suitable anesthetic for chronic focal cerebral ischemia studies in the rat: a comparative study. *Brain Res, 1191*, 157-167.

Ma, J., & Leung, L. S. (2010). Kindled seizure in the prefrontal cortex activated behavioral hyperactivity and increase in accumbens gamma oscillations through the hippocampus. *Behav Brain Res, 206*(1), 68-77.

Macé, E., Montaldo, G., Cohen, I., Baulac, M., Fink, M., & Tanter, M. (2011). Functional ultrasound imaging of the brain. *Nat Methods, 8*(8), 662-664.

Manninen, P. H., Burke, S. J., Wennberg, R., Lozano, A. M., & El Beheiry, H. (1999). Intraoperative localization of an epileptogenic focus with alfentanil and fentanyl. *Anesth Analg, 88*(5), 1101-1106.

McBurney, J. W., Teiken, P. J., & Moon, M. R. (1993). Propofol for treating status epilepticus. *J Epilepsy, 7*(1), 21-22.

Muñoz, H. R., Altermatt, F. R., González, J. A., & León, P. J. (2005). The effect of different isoflurane-fentanyl dose combinations on early recovery from anesthesia and postoperative adverse effects. *Anesth Analg, 101*(2), 371-376.

Nair, D. R. (2016). Management of Drug-Resistant Epilepsy. *Continuum (Minneap Minn), 22*(1 Epilepsy), 157-172.

Nelson, T. S., Suhr, C. L., Lai, A., Halliday, A. J., Freestone, D. R., McLean, K. J., . . . Cook, M. J. (2010). Seizure severity and duration in the cortical stimulation model of experimental epilepsy in rats: a longitudinal study. *Epilepsy Res, 89*(2-3), 261-270.

Nersesyan, H., Hyder, F., Rothman, D. L., & Blumenfeld, H. (2004). Dynamic fMRI and EEG recordings during spike-wave seizures and generalized tonic-clonic seizures in WAG/Rij rats. *J Cereb Blood Flow Metab, 24*(6), 589-599.

Ngugi, A. K., Bottomley, C., Kleinschmidt, I., Sander, J. W., & Newton, C. R. (2010). Estimation of the burden of active and life-time epilepsy: a meta-analytic approach. *Epilepsia, 51*(5), 883-890.

Norwood, B. A., Bumanglag, A. V., Osculati, F., Sbarbati, A., Marzola, P., Nicolato, E., . . . Sloviter, R. S. (2010). Classic hippocampal sclerosis and hippocampal-onset epilepsy produced by a single "cryptic" episode of focal hippocampal excitation in awake rats. *J Comp Neurol, 518*(16), 3381-3407.

Nowell, M., Miserocchi, A., McEvoy, A. W., & Duncan, J. S. (2014). Advances in epilepsy surgery. *J Neurol Neurosurg Psychiatry, 85*(11), 1273-1279.

Osawa, S., Iwasaki, M., Hosaka, R., Matsuzaka, Y., Tomita, H., Ishizuka, T., . . . Mushiake, H. (2013). Optogenetically Induced Seizure and the Longitudinal Hippocampal Network Dynamics. *PloS One, 8*(4), e60928.

Pathan, H., & Williams, J. (2012). Basic opioid pharmacology: an update. *Br J Pain, 6*(1), 11-16.

Paxinos, G., & Watson, C. (2013). *The rat brain in stereotaxic coordinates* (7th ed.). San Diego: Academic Press.

Peeters, R. R., Tindemans, I., De Schutter, E., & Van der Linden, A. (2001). Comparing BOLD fMRI signal changes in the awake and anesthetized rat during electrical forepaw stimulation. *Magn Reson Imaging, 19*(6), 821-826.

Peña, F., & Tapia, R. (2000). Seizures and neurodegeneration induced by 4-aminopyridine in rat hippocampus in vivo: role of glutamate- and GABA-mediated neurotransmission and of ion channels. *Neuroscience, 101*(3), 547-561.

Polásek, R., Kubová, H., Slamberová, R., Mares, P., & Vorlícek, J. (1996). Suppression of cortical epileptic afterdischarges in developing rats by anticonvulsants increasing GABAergic inhibition. *Epilepsy Rev, 25*(3), 117-184.

Rao, A. (2000). *Electrical impedance tomography of brain activity: studies into its accuracy and physiological mechanisms.* PhD thesis: University College London.

Renvall, V., Nangini, C., & Hari, R. (2014). All that glitters is not BOLD: inconsistencies in functional MRI. *Sci Rep, 4*, 3920.

Rosenbluth, A., & Cannon, W. B. (1942). Cortical responses to electrical stimulation. *Am J Physiol, 135*, 690-741.

Sanabria, E. R., D'Andrea Vieira, I., da Silveira Pereira, M. F., Faria, L. C., da Silva, A. C., Cavalheiro, E. A., & da Silva Fernandes, M. J. (2006). Pro-epileptic effect of alfentanil in rats subjected to pilocarpine-induced chronic epilepsy. *Brain Res Bull, 69*(5), 535-545.

Sayin, U., Osting, S., Hagen, J., Rutecki, P., & Sutula, T. (2003). Spontaneous seizures and loss of axo-axonic and axo-somatic inhibition induced by repeated brief seizures in kindled rats. *J Neurosci, 23*(7), 2759-2768.

Schuele, S. U., & Lüders, H. O. (2008). Intractable epilepsy: management and therapeutic alternatives. *Lancet Neurol, 7*(6), 514-524.

Schwark, W. S., Frey, H. H., & Czuczwar, S. J. (1986). Effect of opiates on the parameters of seizures in rats with full amygdaloid-kindled convulsions. *Neuropharmacology, 25*(8), 839-844.

Segev, G., Yas-Natan, E., Shlosberg, A., & Aroch, I. (2006). Alpha-chloralose poisoning in dogs and cats: A retrospective study of 33 canine and 13 feline confirmed cases. *Vet J, 172*(1), 109-113.

Shepherd, G. M. (2004). *The synaptic organisation of the brain* (5th ed.). New York: Oxford University Press.

Shorvon, S., & Ferlisi, M. (2011). The treatment of super-refractory status epilepticus: a critical review of available therapies and a clinical treatment protocol. *Brain, 134*(Pt 10), 2802-2818.

Sleigh, J. W., Vizuete, J. A., Voss, L., Steyn-Ross, A., Steyn-Ross, M., Marcuccilli, C. J., & Hudetz, A. G. (2009). The Electrocortical Effects of Enflurane: Experiment and Theory. *Anesth Analg, 109*(4), 1253-1262.

Smith, M., Wilcox, K. S., & White, H. S. (2007). Discovery of antiepileptic drugs. *Neurotherapeutics, 4*(1), 12-17.

Spencer, S. S. (1996). Long-term outcome after epilepsy surgery. *Epilepsia, 37*(9), 807-813.

Spencer, S. S., Berg, A. T., Vickrey, B. G., Sperling, M. R., Bazil, C. W., Shinnar, S., . . . Frobish, D. (2003). Initial outcomes in the Multicenter Study of Epilepsy Surgery. *Neurology, 61*(12), 1680-1685.

Stecker, M. M., Kramer, T. H., Raps, E. C., O'Meeghan, R., Dulaney, E., & Skaar, D. J. (1998). Treatment of refractory status epilepticus with propofol: clinical and pharmacokinetic findings. *Epilepsia, 39*(1), 18-26.

Téllez-Zenteno, J. F., & Hernández-Ronquillo, L. (2012). A Review of the Epidemiology of Temporal Lobe Epilepsy. *Epilepsy Res Treat, 2012*, 630853.

Tempelhoff, R., Modica, P. A., Bernardo, K. L., & Edwards, I. (1992). Fentanyl-induced electrocorticographic seizures in patients with complex partial epilepsy. *J Neurosurg, 77*(2), 201-208.

Tsurugizawa, T., Ciobanu, L., & Le Bihan, D. (2013). Water diffusion in brain cortex closely tracks underlying neuronal activity. *Proc Natl Acad Sci U S A, 110*(28), 11636-11641.

van Luijtelaar, E. L., Drinkenburg, W. H., van Rijn, C. M., & Coenen, A. M. (2002). Rat models of genetic absence epilepsy: what do EEG spike-wave discharges tell us about drug effects? *Methods Find Exp Clin Pharmacol, 24*(Suppl D), 65-70.

Velísek, L., & Mares, P. (2004). Hippocampal afterdischarges in rats. I. Effects of antiepileptics. *Physiol Res, 53*(4), 453-461.

Vicedomini, J. P., & Nadler, J. V. (1987). A model of status epilepticus based on electrical stimulation of hippocampal afferent pathways. *Exp Neurol, 96*(3), 681-691.

Vongerichten, A. N., Sato Dos Santos, G. S., Aristovich, K., Avery, J., McEvoy, A., Walker, M., & Holder, D. S. (2016). Characterisation and imaging of cortical impedance changes during interictal and ictal activity in the anaesthetised rat. *Neuroimage, 124*(Pt A), 813-823.

Walker, M. C., Perry, H., Scaravilli, F., Patsalos, P. N., Shorvon, P. N., & Jefferys, J. G. (1999). Halothane as a neuroprotectant during constant stimulation of the perforant path. *Epilepsia, 40*(3), 359-364.

Weir, C. J., Mitchell, S. J., & Lambert, J. J. (2017). Role of GABAA receptor subtypes in the behavioural effects of intravenous general anaesthetics. *Br J Anaesth, 119*(suppl_1), i167-i175.

Wang, Y., Xu, C., Xu, Z., Ji, C., Liang, J., Wang, Y., . . . Chen, Z. (2017). Depolarized GABAergic Signaling in Subicular Microcircuits Mediates Generalized Seizure in Temporal Lobe Epilepsy. *Neuron, 95*(1), 92-105.

Winters, W. D., & Spooner, C. E. (1966). A neurophysiological comparison of alpha-chloralose with gamma-hydroxybutyrate in cats. *Electroencephalogr Clin Neurophysiol, 20*(1), 83-90.

Wood, P. R., Browne, G. P., & Pugh, S. (1988). Propofol infusion for the treatment of status epilepticus. *Lancet, 1*(8583), 480-481.

Zeng, H., & Madisen, L. (2012). Mouse transgenic approaches in optogenetics. *Prog Brain Res, 196*, 192-213.